

AD-A040 294

NAVAL AIR PROPULSION TEST CENTER TRENTON N J PROPULS--ETC F/G 21/5  
ROTOR BURST PROTECTION PROGRAM: EXPERIMENTATION TO PROVIDE GUID--ETC(U)  
MAR 77 G J MANGANO, J T SALVINO, R A DELUCIA

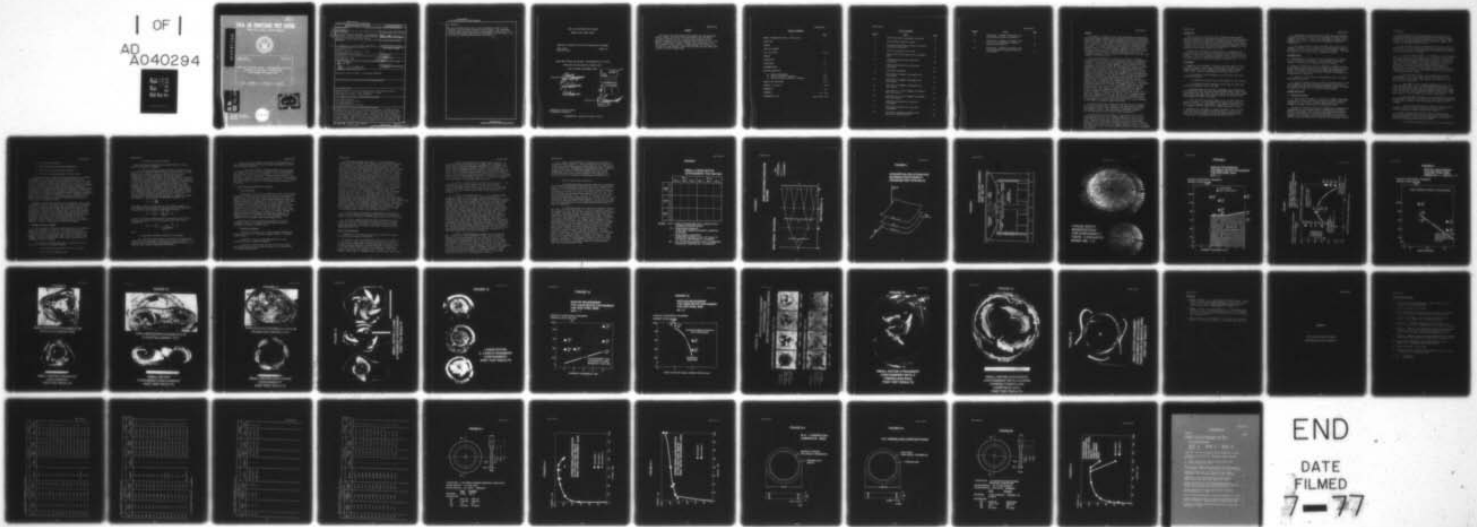
UNCLASSIFIED

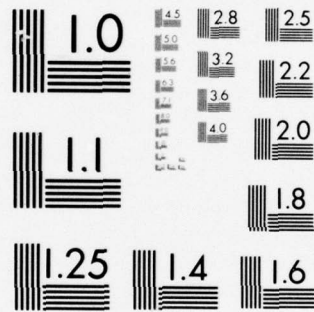
NAPTC-PE-98

NASA-CR-135166

NL

| OF |  
AD  
A040294





MICROCOPY RESOLUTION TEST CHART  
NATIONAL BUREAU OF STANDARDS-1963-A

72  
D-5

# NAVAL AIR PROPULSION TEST CENTER

TRENTON, NEW JERSEY 08628

ADA 040294



NAPTC-PE-98  
 NASA-CR-135166

MARCH 1977

ROTOR BURST PROTECTION PROGRAM: EXPERIMENTATION TO PROVIDE  
 GUIDELINES FOR THE DESIGN OF TURBINE ROTOR  
 BURST FRAGMENT CONTAINMENT RINGS

By G. J. MANGANO, J. T. SALVINO & R. A. DeLUCIA

AD No. \_\_\_\_\_  
DDC FILE COPY,

DDC  
JUN 8 1977  
B

APPROVED FOR PUBLIC  
RELEASE: DISTRIBUTION  
UNLIMITED



UNCLASSIFIED

SECURITY CLASSIFICATION OF THIS PAGE (When Data Entered)

REPORT DOCUMENTATION PAGE		READ INSTRUCTIONS BEFORE COMPLETING FORM
1. REPORT NUMBER 14 NAPTC-PE-98	2. GOVT ACCESSION NO.	3. RECIPIENT'S CATALOG NUMBER
4. TITLE (and Subtitle) 6 ROTOR BURST PROTECTION PROGRAM: EXPERIMENTATION TO PROVIDE GUIDELINES FOR THE DESIGN OF TURBINE ROTOR BURST FRAGMENT CONTAINMENT RINGS.	5. TYPE OF REPORT & PERIOD COVERED 9 FINAL REPORT, 1972-1976, 8 PERFORMING ORG. REPORT NUMBER	
7. AUTHOR(s) 10 G. J. Mangano, J. T. Salvino & R. A. DeLucia	8. CONTRACT OR GRANT NUMBER(s) NASA DPR C-41581-B, MOD. 6	
9. PERFORMING ORGANIZATION NAME AND ADDRESS Commanding Officer Naval Air Propulsion Test Center (PE4) Trenton, New Jersey 08628	10. PROGRAM ELEMENT, PROJECT, TASK AREA & WORK UNIT NUMBERS None	
11. CONTROLLING OFFICE NAME AND ADDRESS National Aeronautics and Space Administration Lewis Research Center Cleveland, Ohio 44135	11	12. REPORT DATE March 1977
14. MONITORING AGENCY NAME & ADDRESS (if different from Controlling Office) 18 NASA 19 CR-135166	12	13. NUMBER OF PAGES 51 p.
15. SECURITY CLASS. (of this report) UNCLASSIFIED		15a. DECLASSIFICATION/DOWNGRADING SCHEDULE
16. DISTRIBUTION STATEMENT (of this Report) APPROVED FOR PUBLIC RELEASE: DISTRIBUTION UNLIMITED		
17. DISTRIBUTION STATEMENT (of the abstract entered in Block 20, if different from Report)		
18. SUPPLEMENTARY NOTES National Aeronautics and Space Administration, Lewis Research Center, Cleveland, Ohio 44135, Project Manager, A. G. Holms Other report designation: NASA-CR-135166		
19. KEY WORDS (Continue on reverse side if necessary and identify by block number) Rotor Burst Protection Air Transportation and Safety Structural Mechanics Gas Turbine Engine Rotor Failures		
20. ABSTRACT (Continue on reverse side if necessary and identify by block number) Presented are the results of a program of rotor burst containment experimentation that provides guidelines for the design of optimum weight turbine rotor disk fragment containment rings. These guidelines were derived by establishing the relationships between a measure of the ring's capability to contain fragment energy with respect to it's weight (the specific contained fragment energy - SCFE - derived by dividing the rotor burst energy by the weight of ring required to contain this energy) and other significant ring		

UNCLASSIFIED

SECURITY CLASSIFICATION OF THIS PAGE(When Data Entered)

20. ABSTRACT

and rotor variables such as the: rotor tip diameter; number of rotor fragments; and ring radial thickness and axial length. The experiments consisted mainly of bursting 14 and 31 inch diameter turbine rotors into encircling containment rings made from centrifugally cast 4130 steel. Rules are given for achieving optimum weight ring designs.

UNCLASSIFIED

SECURITY CLASSIFICATION OF THIS PAGE(When Data Entered)

NAVAL AIR PROPULSION TEST CENTER  
TRENTON, NEW JERSEY 08628

PROPULSION TECHNOLOGY AND PROJECT ENGINEERING DEPARTMENT

NAPTC-PE-98  
NASA-CR-135166

MARCH 1977

ROTOR BURST PROTECTION PROGRAM: EXPERIMENTATION TO PROVIDE  
GUIDELINES FOR THE DESIGN OF TURBINE ROTOR  
BURST FRAGMENT CONTAINMENT RINGS

Prepared by:

*J. J. Mangano*  
E. J. MANGANO

*J. T. Salvino*  
J. T. SALVINO

*R. A. DeLucia*  
R. A. DeLUCIA

NTIS White Section   
DDC Bufl Section   
UNANNOUNCED   
JUSTIFICATION.....

BY.....  
DISTRIBUTION/AVAILABILITY CODES

Disc. AVAIL. and/or SPECIAL

A		
---	--	--

Approved by:

*R. K. Brumwell*  
R. K. BRUMWELL  
Commander, USN  
Director, PE

APPROVED FOR PUBLIC RELEASE:  
DISTRIBUTION UNLIMITED

AUTHORIZATION: NASA DPR C-41581-B, MOD. 6

NAPTC-PE-98

FORWARD

This report has been prepared by the Naval Air Propulsion Test Center, Trenton, New Jersey under NASA Defense Purchase Request C-41581-B, Modification No. 6 from the Lewis Research Center, National Aeronautics and Space Administration, Cleveland, Ohio 44135. Messrs. Solomon Weiss, Robert D. Siewert and Arthur Holms of the Lewis Research Center served as program managers and technical consultants for this program. Their contributions and help during this program are greatly appreciated.

TABLE OF CONTENTS

	<u>Page</u>
REPORT DOCUMENTATION PAGE -- DD Form 1423	
TITLE PAGE	
FORWARD	
TABLE OF CONTENTS	i
LIST OF FIGURES	ii-iii
SUMMARY	1
INTRODUCTION	2
CONCLUSIONS	2-3
RECOMMENDATIONS	3
PROGRAM DESCRIPTION	3
A. Concept Development	3-5
B. Design Guidelines Synthesis	5-7
C. Test Procedures & Methods Of Analysis	7-8
RESULTS AND DISCUSSION	8-10
FIGURES 1 through 19	11-29
REFERENCES	30
APPENDIX A	A-1 - A-13
DISTRIBUTION LIST	Inside rear cover

LIST OF FIGURES

<u>Figure</u>	<u>Title</u>	<u>Page</u>
1	Small/Large Rotor Containment Test Matrix	11
2	Ring Thickness Variation Scheme	12
3	Conceptual Relationships Between Containment Program Test Variables	13
4	Typical Containment Test Set-Up	14
5	Typical Rotor Modifications For Containment Tests	15
6	SCFE-NF Relationship For Small Rotor Containment	16
7	SCFE-ALR Relationship For Small Rotor Containment	17
8	SCFE-ID <sub>R</sub> Relationship	18
9	Small Rotor 3 Fragment Containment Post Test Results	19
10	Small Rotor 2 Fragment Containment Post Test Results	20
11	Small Rotor 6 Fragment Containment Post Test Results	21
12	Small Rotor 2, 3 and 6 Fragment Containment Post Test Results	22
13	Large Rotor 2, 3 and 6 Fragment Containment Post Test Results	23
14	SCFE-NF Relationship For Large Rotor Containment	24
15	SCFE-ALR Relationship For Large Rotor Containment	25
16	Rotor Burst Fragment Containment Ring Deformation Characteristics	26

<u>Figure</u>	<u>Title</u>	<u>Page</u>
17	Small Rotor 3 Fragment Containment With A Fiberglass Ring Post Test Results	27
18	Small Rotor 3 Fragment Containment With A Boron Carbide/Fiberglass Composite Ring Post Test Results	28
19	Small Rotor 3 Fragment Containment With A Steel/Fiberglass Composite Ring Post Test Results	29

SUMMARY

The program of parametric rotor burst containment experimentation being reported was developed and conducted by the Naval Air Propulsion Test Center (NAPTC) under National Aeronautics and Space Administration (NASA) sponsorship. The program was structured to develop guidelines for the design of optimum weight turbine rotor disk fragment containment rings. The design guidelines were generated by experimentally establishing the relationship between a specific energy variable that provides a measure of ring containment capability, and several select variables which characterize those configurational aspects of the containment rings and rotor fragments that significantly influence the fragment containment process.

The program consisted of a series of rotor burst containment experiments in which rotors of two different diameters were modified to burst at their respective design speeds into various numbers (2, 3 and 6) of pie-sector shaped fragments. These fragments impacted rings made from 4130 cast steel that encircled the rotors at a radial clearance of 0.5 inches (0.0127 m). The ring axial lengths were varied in three discrete steps of 1/2, 1, and 2 times the rim axial length of the rotors used. The radial thicknesses of the rings were varied until fragment containment was achieved, thus establishing the weight of ring required. The results of test provided the guidelines necessary to design an optimum weight steel containment ring for small rotors. The optimum weight ring was 8.6 lbs (3.9 kg) for a 14 inch (0.356 m) diameter rotor having a burst energy of  $10^6$  in-lbs (3511.6 J) at its design speed of 20,000 rpm (2094 rad/s). This weight decreased slightly with the number of fragments generated at burst in the range of from 2 to 6. The results also indicated that the weight of steel ring required to contain the pie-sector fragments from an average size commercial engine turbine rotor (31 inch (0.787 m) diameter) having a burst energy of  $10 \times 10^6$  in-lbs (35116 J) would be in excess of 168 lbs (76.2 kg) for 2 and 3-fragment bursts and in the neighborhood of 150 lbs (68 kg) for a 6-fragment burst. Unlike the small rotor containment ring characteristics, the weight of ring required to contain these larger rotors was clearly dependent on the number of fragments generated at burst.

It was also found that a composite ring made from boron carbide backed with filament wound fiberglass in an epoxy matrix contained the fragments from the small rotor burst at a weight reduction of 30% compared to steel. This represents a significant weight reduction configuration that warrants further exploration.

It would appear from the results of this effort that the steel rings required to contain the fragments generated by the burst of an average size turbine rotor (the larger of the two rotors tested) from a commercial engine would be heavy for aircraft application. However, the use of optimally configured composite rings for fragment containment and partial rings for fragment deflection, which are systems that show great promise for light-weight protection, should be thoroughly investigated.

INTRODUCTION

This is a report on the Rotor Burst Protection Program (RBPP), which is sponsored by the National Aeronautics and Space Administration (NASA) and conducted by the Naval Air Propulsion Test Center (NAPTC). The objective of this program is to develop guidelines for the design of devices that will be used on aircraft to protect passengers and the aircraft structure from the lethal and devastating fragments that are generated by gas turbine engine rotor bursts.

Presented in this report are the results of a parametric test program that was conducted by the NAPTC to provide guidelines for the design of turbine rotor fragment containment rings. This program was a sequel to, and to a large extent guided by, the exploratory testing that was conducted by NAPTC and reported in reference (a).

CONCLUSIONS

1. Regarding the containment of typical, relatively small (14 inch (0.356 m)) diameter, axial flow turbine rotors that burst at their design speeds into various numbers of pie-sector shaped fragments having a total energy of approximately  $10^6$  in-lbs (3511.6 J):

a. Containment of these fragments can be achieved using rings described as follows:

(1) Rings made from 4130 cast steel weighing 8.6 lbs (3.9 kg).

(2) Laminated rings consisting of boron-carbide backed with fiberglass weighing 6.02 lbs (2.71 kg).

b. Optimum weight for the steel containment ring configuration was achieved when the ring axial length was made equal to that of the rotor; making the ring twice or half as long as the rotor axial length resulted in containment rings that were heavier and therefore less than optimum with respect to weight.

c. With the steel ring axial length at its optimum value with respect to weight, the ring thickness and therefore its weight is, for practical purposes, independent of the number (ranging from 2 to 6) of equal pie-sector shaped rotor fragments generated at burst.

2. Regarding the containment of typical relatively large (31 inch (0.787 m)) axial flow turbine rotors that burst at their design speeds into various numbers of pie-sector shaped fragments having a total energy of approximately  $10 \times 10^6$  in-lbs (35116 J):

a. Rings made from relatively brittle 4130 cast-steel weighing in excess of 168 lbs (76.2 kg) will be required to contain 2 and 3 fragment rotor bursts. A ring of the same material weighing in the neighborhood of 150 lbs (68 kg) will be required to contain a 6-fragment burst.

b. The optimum weight of 4130 cast-steel ring required for containment is dependent on the number of pie-sector shaped fragments generated at burst in the range of from 2 to 6 fragments. The weight will increase as the number of such fragments decreases.

#### RECOMMENDATIONS

1. Experimentation and analysis should be continued on a limited basis to establish the baseline or reference steel ring weight required to contain 2 and 3 fragment large rotor bursts.

2. Because the weight of steel rings required to contain the pie-sector shaped burst fragments from an average size commercial engine turbine rotor appears to be excessively high, the following two facets of rotor burst protection should be further investigated and design guidelines developed:

a. The use of multi-layered, multi-material rings for containment applications, and

b. The use of partial rings to control the trajectories of rotor burst fragments (directing them away from the more vital areas of the aircraft into the less or negligibly sensitive areas) as a means of providing a "degree" of protection at reduced weight.

#### PROGRAM DESCRIPTION

##### A. Concept Development

1. The program of parametric turbine rotor fragment containment testing that is being reported was structured to develop empirical guidelines for the design of minimum weight turbine rotor disk fragment containment rings made from a monolithic metal.

The empirical design guidelines were generated by experimentally establishing the relationship between a variable that provides a measure of containment ring capability and several other variables that both characterized the configurational aspects of the rotor fragments and containment ring; and had been found from exploratory testing to have had significant influence on the containment process.

The variable that provided this measure of containment ring potential or capability was termed the Specific Contained Fragment Energy (SCFE) and was derived by dividing the rotor fragment energy at burst by the ring weight required to contain this energy. The SCFE was the dependent variable of test.

2. The four ring and rotor characteristics that were chosen for test because of their suspected influence on the containment process, and varied during test to establish what this influence was (as measured by the SCFE) were as follows:

a. The ring inner diameter. Two diameters, one approximately twice as large as the other (31.64 and 15 inches) were used for test with rotors having correspondingly larger and smaller tip diameters (the CWJ65 and GET58 engine turbine rotors having tip diameters of 30.64 (.778 m) and 14 (0.356 m) inches, respectively). The burst energies of these rotors at their nominal design speeds were  $10 \times 10^6$  and  $10^6$  in-lbs (35116 and 3511.6J) for the larger and smaller rotor, respectively. Burst fragment energy (speed) was held constant from test to test as a function of rotor size; the larger rotor having the higher energy.

b. The ring axial length. Three lengths were used that corresponded to 1/2, 1 and 2 times the rim axial lengths of the large and small rotors which were nominally 1.25 and 1 inch (.032 and .0254 m), respectively.

c. The number of rotor fragments generated at burst. The rotors were modified to fail at their respective design speeds of 8,500 rpm (890. rad/s) (J65 rotor) and 20,000 rpm (2094 rad/s) (T58 rotor) and produce pie-sector shaped fragments having included angles of  $60^\circ$  (1.0472 rad),  $120^\circ$  (2.0944 rad) and  $180^\circ$  (3.1416 rad). These were termed 6, 3 and 2-fragment rotor bursts, respectively.

d. The ring radial thickness. The ring thickness was varied until fragment containment was achieved for the different combinations of ring (rotor) diameter; ring axial length; and number of rotor fragments.

The resultant test matrix for this test program is shown in Figure 1; and the procedure for ring thickness variation to achieve containment is shown schematically in Figure 2.

3. Other variables which would, in some way, influence the magnitude and orientation of the forces that create the deformations and displacements of the ring and rotor fragments, and therefore govern the containment process are as follows:

a. The mechanical properties of the rotor and ring materials.

- b. The fragment velocities.
- c. The fragment masses and mass distributions.
- d. The rotor-to-ring radial tip clearance.
- e. The rotor tip-to-hub diameter or radius ratio.

Although these factors would significantly influence the containment process, with the exception of the ring material used for containment, the variability of these factors, as a function of rotor size, are constrained within relatively narrow limits by the dictates of rotor aerothermal and structural design. For all practical purposes then, for a given rotor size, these factors would be essentially invariable and the results generated by the experiments conducted would be generally applicable to all turbines as a function of rotor size. This would be so because the experimental scheme presented incorporates, either purposely through the variables of test or inherently because actual rotors are used, all of the factors that could (with the exception of ring material properties) significantly influence the rotor fragment containment process.

Although the mechanical properties of the materials used to make a containment ring can vary widely and are considered to be important factors in containment ring design, the ring material used in most of the tests conducted was the same from one test to another. The material was 4130 cast steel. This was done to generate a baseline for materials comparison in subsequent tests, and to establish the effects of the other variables on the containment process exclusive of material influences. Later when these effects are firmly established, the influence of ring materials will be more fully explored. In fact, during the tests conducted the use of composite rings as containment devices were cursorily investigated.

#### B. Design Guidelines Synthesis

1. The conceptual functional relationship between the dependent (SCFE) and independent ( $t$ , ALR, NF, ID) variables of test are presented conceptually in Figure 3. Once these relationships are established through test, they provide all the information that is needed to design an optimum weight steel ring for a turbine rotor fragment containment application. Given these relationships, the procedure would be as follows:

a. Three basic things would have to be known about the rotor to proceed with the design analysis:

- (1) The kinetic energy ( $KE_R$ ) of the rotor at burst
- (2) The rotor tip diameter, and

## (3) The rotor rim axial length.

These are characteristics that are usually known or can be easily calculated by a designer.

b. The relationships between the SCFE, the number of fragments and rotor diameter, with the ratio of ring to rotor rim axial length as the parameter, provide an indication of the worst combination of burst conditions for the size rotor being considered; i.e., the lowest SCFE. For a given analysis, this value of SCFE would be obtained from the curves in Figure 3 (or equations derived from regression analyses of the data points developed through test) for the size rotor being considered; the number of rotor fragments that result in producing the most adverse containment condition with respect to weight of ring (the lowest SCFE value in the SCFE-NF plane; and the optimum ring to rotor rim axial length ratio ( $L_{RG}/L_{RT} \cong ALR$ )), which is represented by the highest contour line. The SCFE value that is obtained by this exercise is divided into the total anticipated energy of the rotor to yield the optimum (lowest) weight steel ring that will be required to contain the fragments. This procedure is expressed in equation (1).

$$(1) \quad W_t = \frac{KER}{SCFE}$$

The weight so derived is then used in the following equation (2) which expresses the thickness of ring required for containment as a function of all the other known dimensional variables.

$$(2) \quad t = \left[ R_i^2 + \frac{W_t}{\rho \pi L_{RG}} \right]^{1/2} - R_i$$

Of course the value of weight derived in equation (1) can be substituted in equation (2) to yield perhaps a more useful form; equation (2a)

$$(2a) \quad t = \left[ R_i^2 + \frac{KER}{\rho \pi L_{RG} SCFE} \right]^{1/2} - R_i$$

where

$t$  = ring radial thickness required for containment

$R_i$  = ring inner radius, which, for practical considerations, equals the rotor tip radius because rotor-to-casing operational clearances and considerations of minimum ring weight dictate that the ring and rotor radius be equivalent as possible.

LRG = ring axial length: Derived by the multiplication of the optimum ALR (parameter of highest contour in Figure 3) and the rotor rim axial length LRT.

c. This data synthesis and design analysis would provide the lightest weight steel ring configuration (ID, radial thickness, and axial length) that would be needed to contain the fragments generated by a turbine rotor burst of known size and energy. The analysis is generally applicable to axial flow turbines from aircraft gas turbine engines because, as mentioned previously, of the inherent operational and configurational similarities between turbines of a given size.

#### C. Test Procedures and Methods of Analysis

##### 1. Test Procedures

Testing was conducted in the NAPTC Rotor Spin Facility (RSF), the detailed capabilities and description of which are contained in reference (b). The test set-up and procedures were basically the same for each test conducted: Rings being evaluated for their containment capability as measured by the SCFE were sandwiched between rigid steel plates and positioned so that they concentrically encircled rotors that were vertically suspended (plane of rotation horizontal) in the spin chamber from the output shaft of the air turbine motor used to spin the rotors to their burst speed. This set-up is shown in Figure 4. The radial tip clearance between the rotor and ring was maintained at 0.50 inch (1.27 cm). The two different size rotors described previously were modified, as shown in Figure 5, to fail into 2, 3 and 6 pie-sector shaped fragments at their nominal operational design speeds.

During test, the spin chamber was evacuated to a vacuum pressure of 10mm Hg to minimize the drive power required to accelerate the rotors to burst speed.

##### 2. Methods of Analysis

Because of the nature of the test program conducted, the analysis of results was relatively straight forward; it depended on two things:

a. Whether or not the ring being subjected to test contained the rotor fragments generated.

b. And if it did contain, what was the associated ring SCFE (by definition no SCFE could be derived for a ring that did not contain the fragments).

As previously mentioned, the SCFE for a ring is derived by dividing the rotor fragment burst energy by the ring weight required for containment. For the tests conducted, two axial flow turbine rotor configurations having different tip diameters (14 and 30.64 inches) bursting at their respective operational design speeds (20,000 and 8,500 rpm) were used. Therefore, from test to test, the rotor burst energy was held constant as a function of rotor size. However, variations in burst energy for a given rotor size did occur during test because of small unpredictable variations in rotor burst speed. These variations stemmed from such factors as: material property scatter; dimensional tolerance differences; flaws or cracks (scrap turbine rotors from high time military engines were used); and other such inherent and induced rotor to rotor anomalies. To account for these "experimental" variations in analyzing the burst test results, the policy was adopted whereby results which had a speed variation greater than  $\pm 2.5\%$  of the design burst speed were not used for analytical purposes; i.e., assessment of a ring's SCFE. The reason for not using the results of a low burst speed (and therefore low energy) test is obvious: It would mistakenly give a lower and therefore erroneously conservative SCFE value for a particular ring configuration. The reason for rejecting the results of a higher burst speed was more subtle and was based on the fact that materials exhibit strain rate sensitivity. Under singularly optimum conditions, it might be possible to derive an erroneously high SCFE from a higher than "rated" burst speed because of a favorable material rate sensitivity. This would indicate that a lighter than required ring would be suitable for containment when in fact at rated speed it would not.

3. In this report, the results of analysis will be presented graphically by indicating the range of SCFE based on the acceptable speed variation ( $\pm 2.5\%$ ) and the SCFE based on the actual burst speed.

4. The other element beside speed that established the rotor energy at burst was the mass moment of inertia of the two turbine rotors used for test. The values of inertia for each rotor were determined experimentally using the well known torsional pendulum method (reference c).

#### RESULTS AND DISCUSSION

A compendium of the pertinent test and calculated data used in this report are presented in Appendix A.

The results of test are presented in plotted form in Figures 6, 7, 8, 14 and 15. These plots are actually plane sections of the conceptual three dimensional (variable) plot shown in Figure 3, but in these instances using the test data developed. The intent here is to clearly show, where possible, the functional relationship between the SCFE and the significant test variables: inner ring diameter (ID<sub>r</sub>); number of fragments (NF); and ring axial length (ALR).

a. SCFE - NF Relationship for Small Rotors; Figure 6. It can be seen from these curves that for small rotor containment the SCFE is for all practical purposes independent of the number of pie-sector shaped fragments generated at burst. This indicates that rings of the same weight would be required for containment regardless of the number of fragments generated at rotor burst in the range of from 2 to 6 fragments and having a total (translational and rotational) energy content of approximately  $10^6$  in-lbs. A corollary to this would be that a worst fragment number condition for small rotor containment with respect to ring weight does not exist.

b. SCFE - ALR Relationship for Small Rotors; Figure 7. The relationship shown in this Figure indicates that an optimum value for ring axial length exists. For the size rotor tested, an optimum lightweight ring for containment is derived when the axial length of the ring is made equal to that of the rotor; that is where  $ALR = 1$ .

c. SCFE -  $ID_R$  Relationship for 2, 3 and 6 Fragment Bursts at  $ALR = 1$ ; Figure 8. First of all, these relationships are incomplete except for the 6-fragment data because the radial thickness required for large rotor containment of the 2 and 3-fragment bursts exceeded that which was available from inventory (4130 cast steel circular rings with an ID of 31.64 inches (0.804 m) and having a maximum radial thickness of 4.1875 inches (.106 m)). The relationship shown in Figure 8 indicates that the amount of fragment energy that a pound of ring material can contain decreases when the rotor size and energy content increases; that is for the same ring to rotor axial length ratio, ring material, and number of fragments generated at burst, the containment capability of the larger ring, as measured by the SCFE (on a contained energy per unit weight basis) is lower than a small ring. This indicates that the practice of extrapolating small rotor containment ring results to large rotor containment ring applications would be very tenuous. To provide some feel for the ring and fragment distortions that normally accompany the containment process, the post-test conditions of rings and rotors from several selected tests (both contained and uncontained) are shown photographically in Figures 9 through 13.

d. SCFE - NF Relationship for Large Rotor Containment at  $ALR = 1$ ; Figure 14. The relationship in this figure, though not definitive because containment was not achieved for the 2 and 3 fragment burst, indicates that the SCFE is dependent on the number of fragments (NF) generated at burst. This differs from the small rotor results, which indicated that the SCFE and NF were almost independent. The trend of this relationship indicates that the capability of a ring increases as the number of fragments generated increases or in other words, as the number of fragments generated at burst decreases the containment situation with respect to ring weight become more adverse, i.e., more weight is required.

e. SCFE - ALR Relationship for Large Rotor Containment of 2-Fragment Bursts; Figure 15. Only limited tests were conducted to explore this relationship because trends indicated that the weights of ring required for containment were becoming very high. Figure 15 tends to show that an optimum axial length might exist in the neighborhood of  $ALR = 1$ . This is consistent with the results of the small rotor results, which because of the abundance of test data, was more conclusive in indicating an optimum  $ALR = 1$ .

f. General Observations and Results:

(1) Comparison Between Large and Small Rotor Containment Ring Deformation/Displacement Characteristics During Fragment Impact: Figure 16 shows high-speed photographic results that depict the mechanics of large and small rotor containment in which a 3-fragment rotor burst is involved. It can be seen from these data that the gross deformations and displacements experienced by the steel rings are quite independent of size. In fact, in a general sense, the deformation/displacement characteristics for the large and small rotor containment rings are approximately identical. On the basis of this data, it was anticipated that a functional relationship between SCFE and rotor diameter/ring ID could be experimentally derived and be generally applicable.

(2) Exploratory Tests of a Small Rotor Composite Containment Ring: Data for these tests can be found in Appendix A under test numbers 143, 144, 183 and 208. These tests were conducted using the smaller T58 engine turbine rotors modified to burst into three fragments at their design speed of 20,000 rpm and impact concentrically, encircling rings that were made from three types of materials or material configurations: (a) filament wound fiberglass in an epoxy matrix; (b) circular boron carbide segments backed by filament wound fiberglass in an epoxy matrix; and (c) a segmented, hardened 4130 steel ring backed by filament wound fiberglass in an epoxy matrix. The fiberglass and steel-fiberglass rings did not contain the fragments; however, the boron carbide-fiberglass ring did contain at a weight savings of 30% over an optimally configured steel ring subjected to identical burst conditions. Post-test photographs of these rings are shown in Figures 17 through 19. On the basis of these exploratory tests, it appears that composite rings may serve to reduce the weight penalty associated with rotor disk fragment containment. To determine what these weight reductions might be, will require an extensive program of experimentation using multi-layered material rings.

**FIGURE 1**

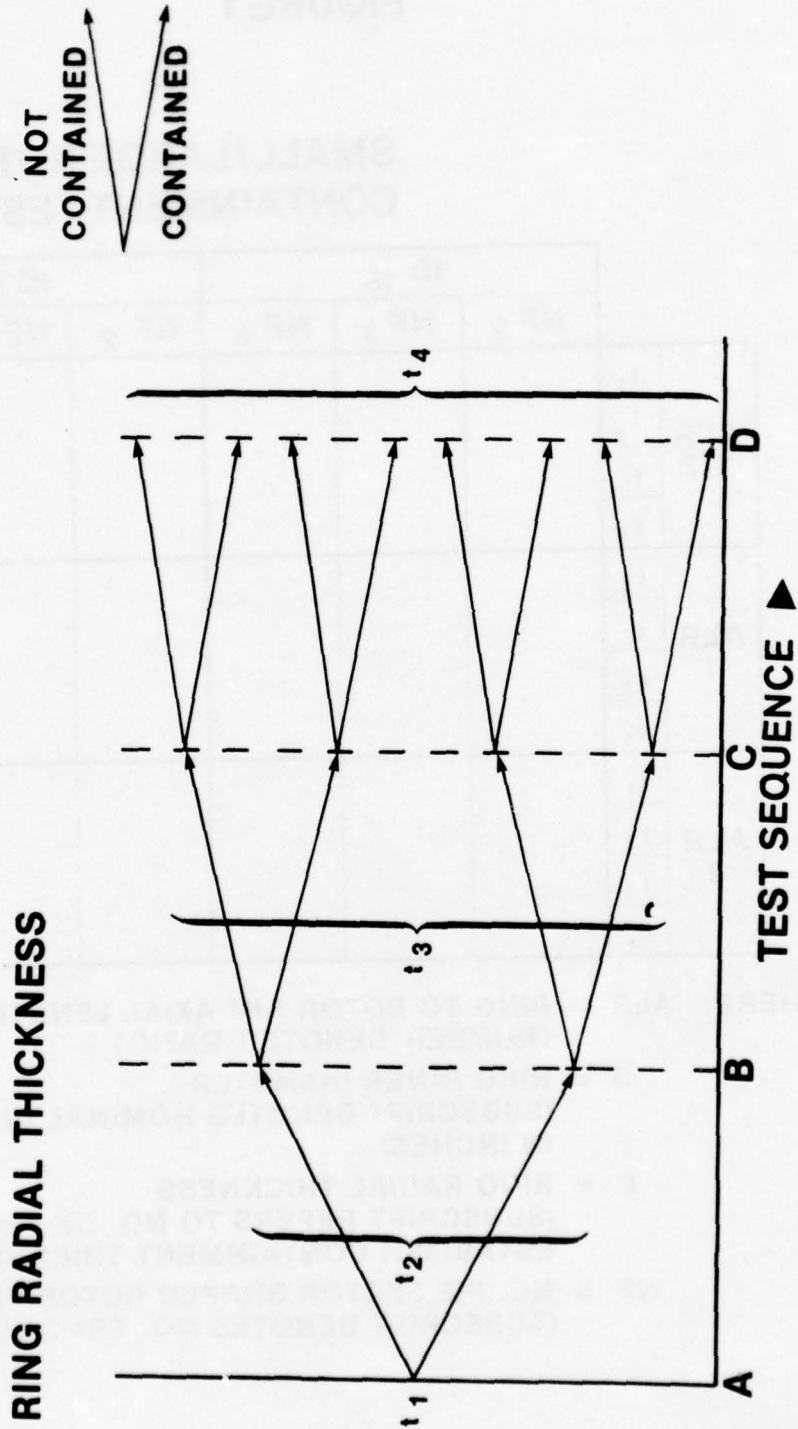
**SMALL/LARGE ROTOR  
CONTAINMENT TEST MATRIX**

		ID 15			ID 32		
		NF 2	NF 3	NF 6	NF 2	NF 3	NF 6
ALR 1/2	t <sub>1</sub>						
	t <sub>2</sub>						
	t <sub>3</sub>						
	t <sub>4</sub>						
ALR 1	t <sub>1</sub>						
	t <sub>2</sub>						
	t <sub>3</sub>						
	t <sub>4</sub>						
ALR 2	t <sub>1</sub>						
	t <sub>2</sub>						
	t <sub>3</sub>						
	t <sub>4</sub>						

- WHERE:** ALR = RING TO ROTOR RIM AXIAL LENGTH RATIO  
(NUMBER DENOTES RATIO)
- ID = RING INNER DIAMETER  
(SUBSCRIPT DENOTES NOMINAL DIAMETER  
IN INCHES)
- t = RING RADIAL THICKNESS  
(SUBSCRIPT REFERS TO NO. OF TRIALS TO  
ESTABLISH CONTAINMENT THICKNESS)
- NF = NO. PIE SECTOR SHAPED ROTOR FRAGMENTS  
(SUBSCRIPT DENOTES NO. FRAGMENTS)

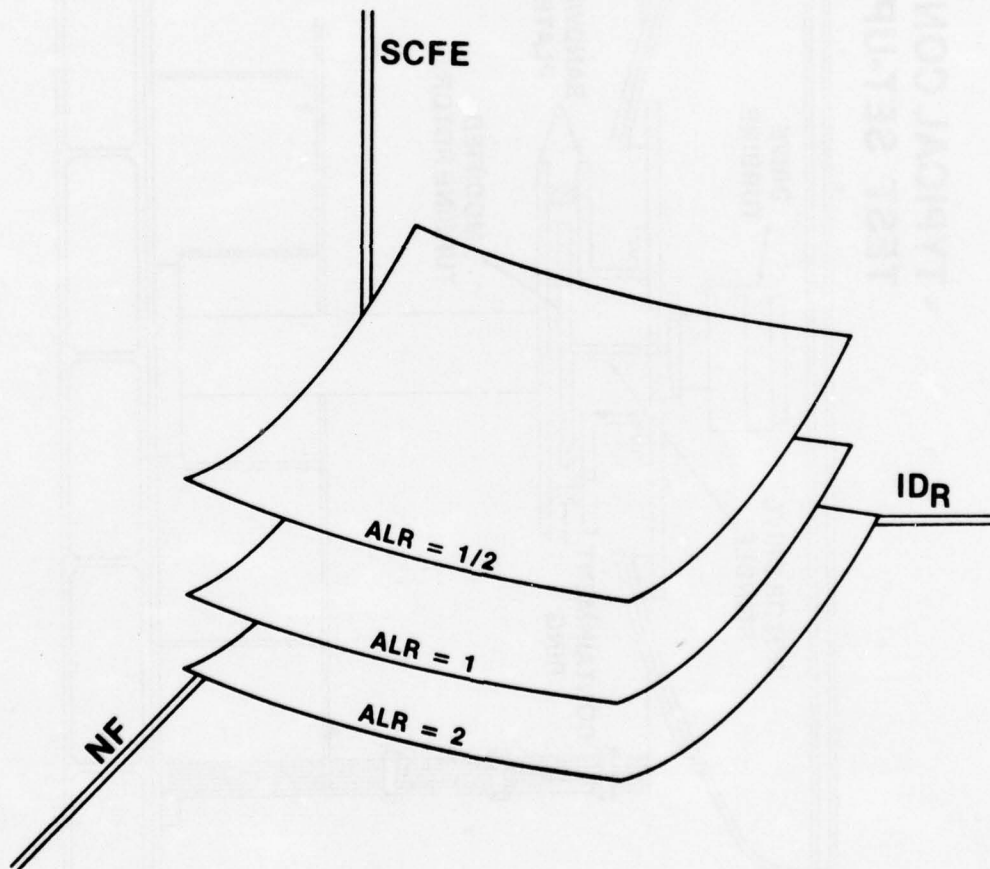
FIGURE 2

**RING THICKNESS VARIATION  
SCHEME**



**FIGURE 3**

**CONCEPTUAL RELATIONSHIPS  
BETWEEN CONTAINMENT  
PROGRAM TEST VARIABLES**



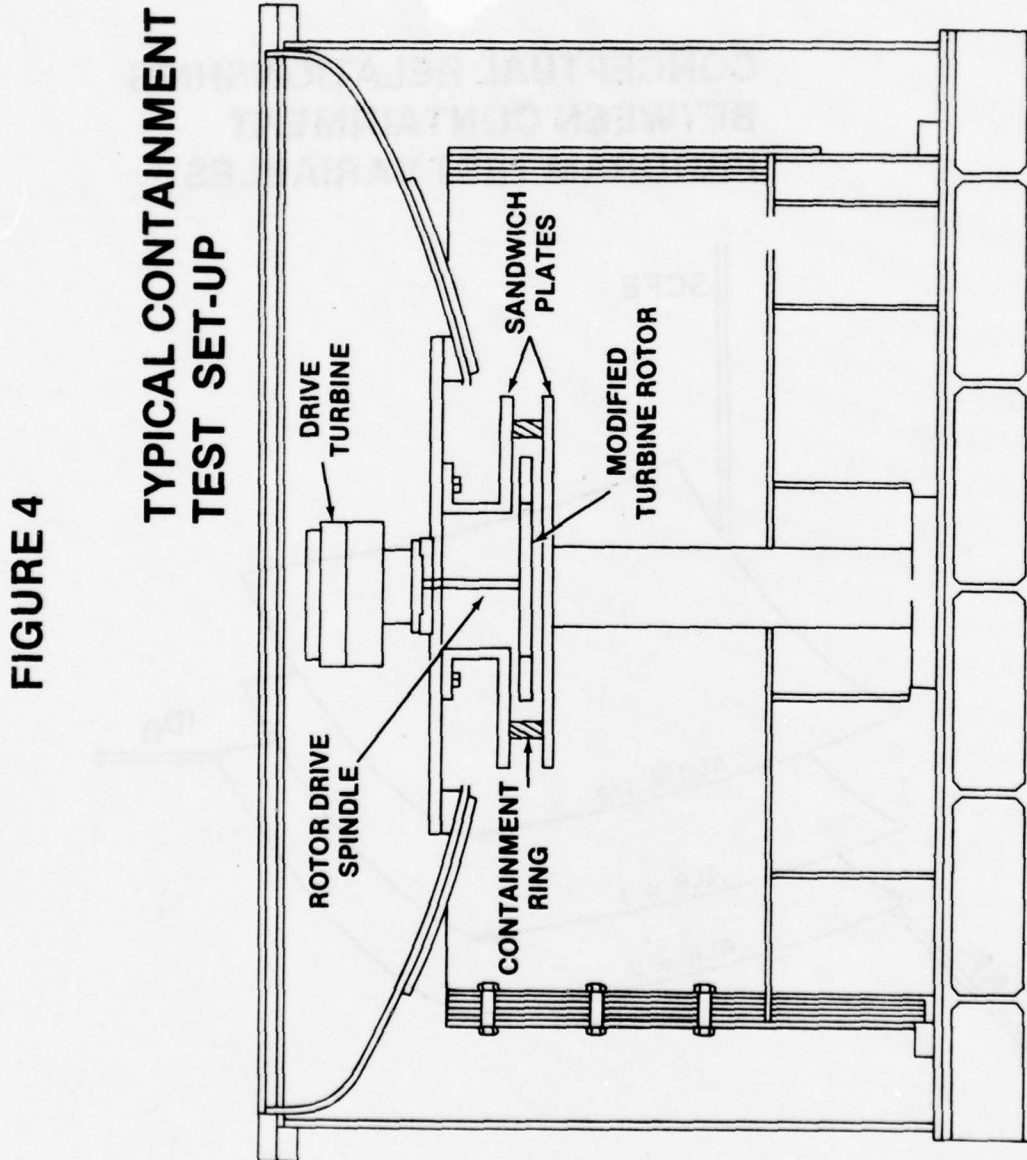
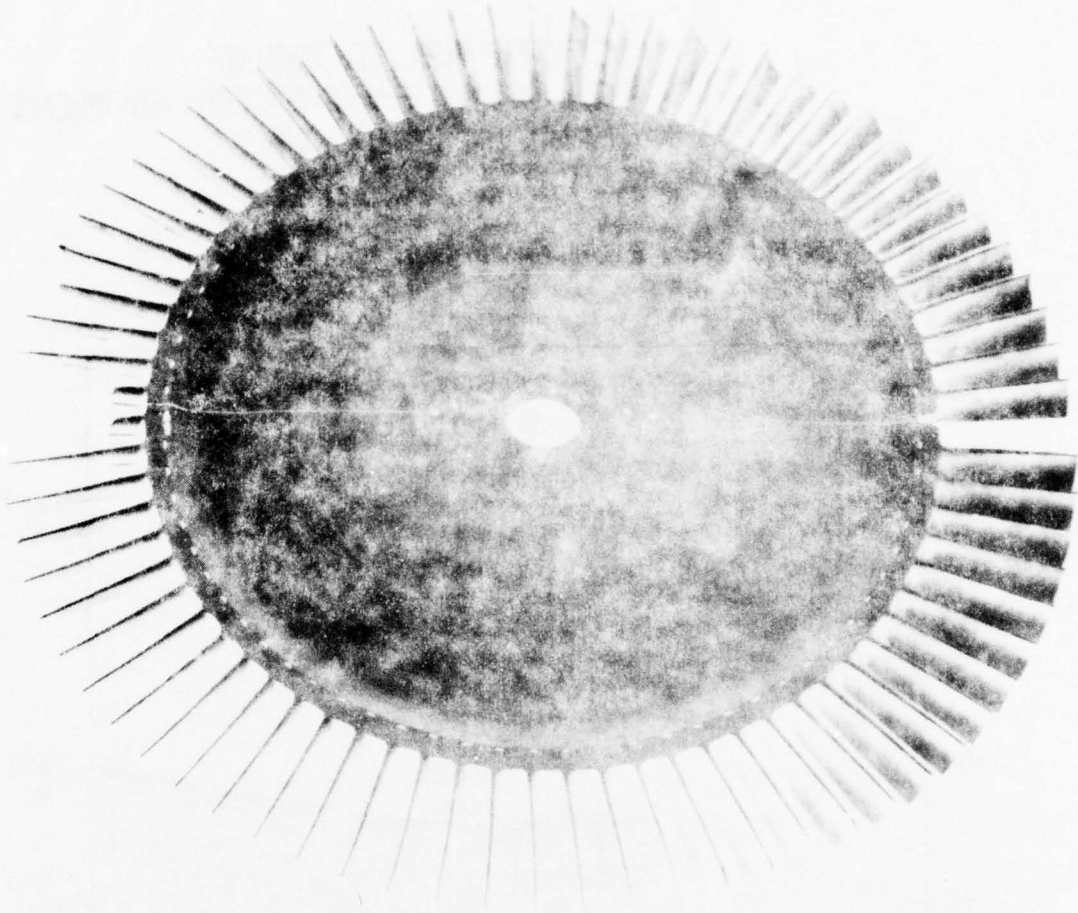


FIGURE 5



**TYPICAL ROTOR  
MODIFICATIONS  
FOR CONTAINMENT  
TESTS; 2-FRAGMENT  
BURST (NF = 2)**

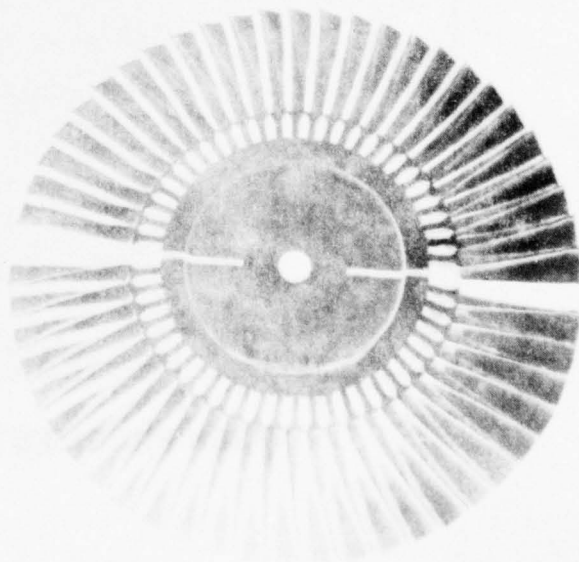


FIGURE 6

SCFE-NF RELATIONSHIP  
FOR SMALL ROTOR CONTAINMENT  
4130 CAST STEEL RING  
ALR = 1

SPECIFIC CONTAINED FRAGMENT  
ENERGY (SCFE)  $\frac{\text{IN-LBS}}{\text{LB}}$

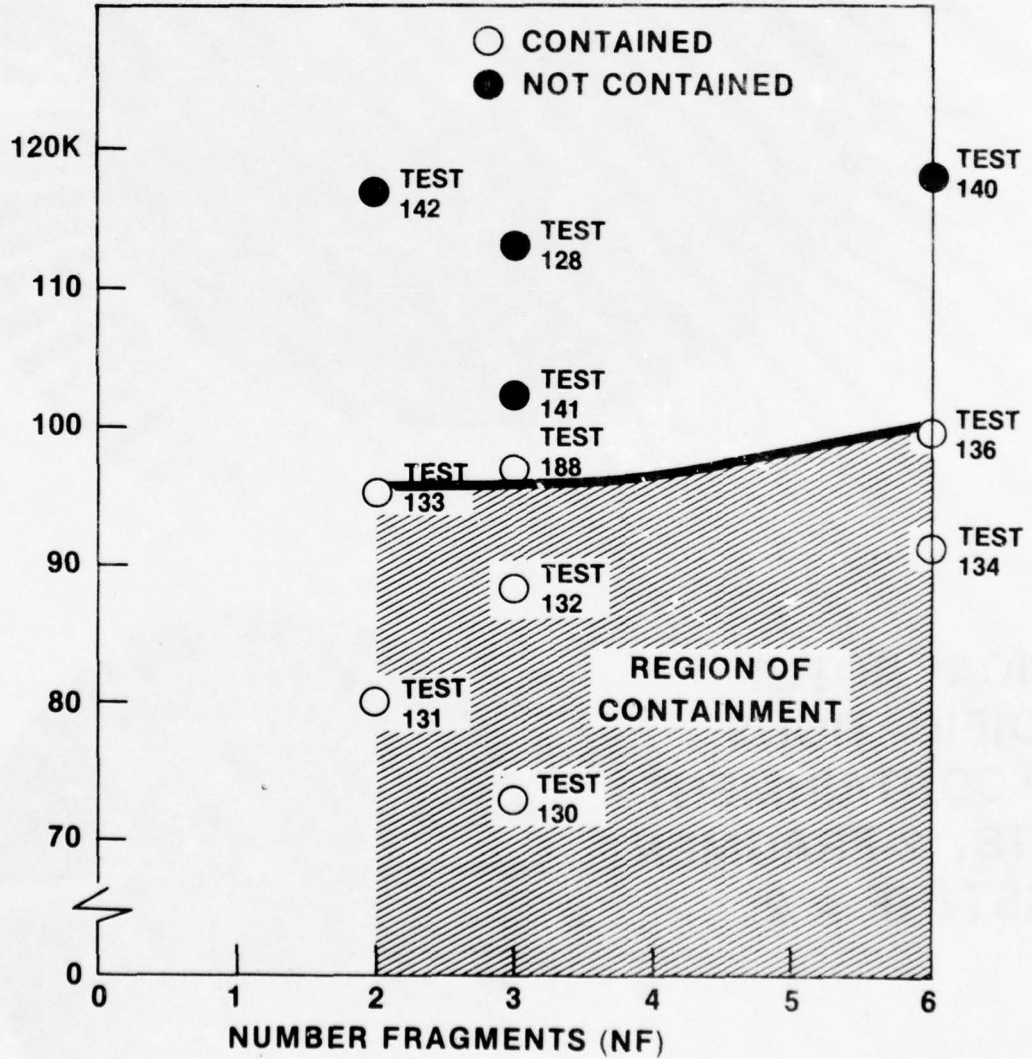
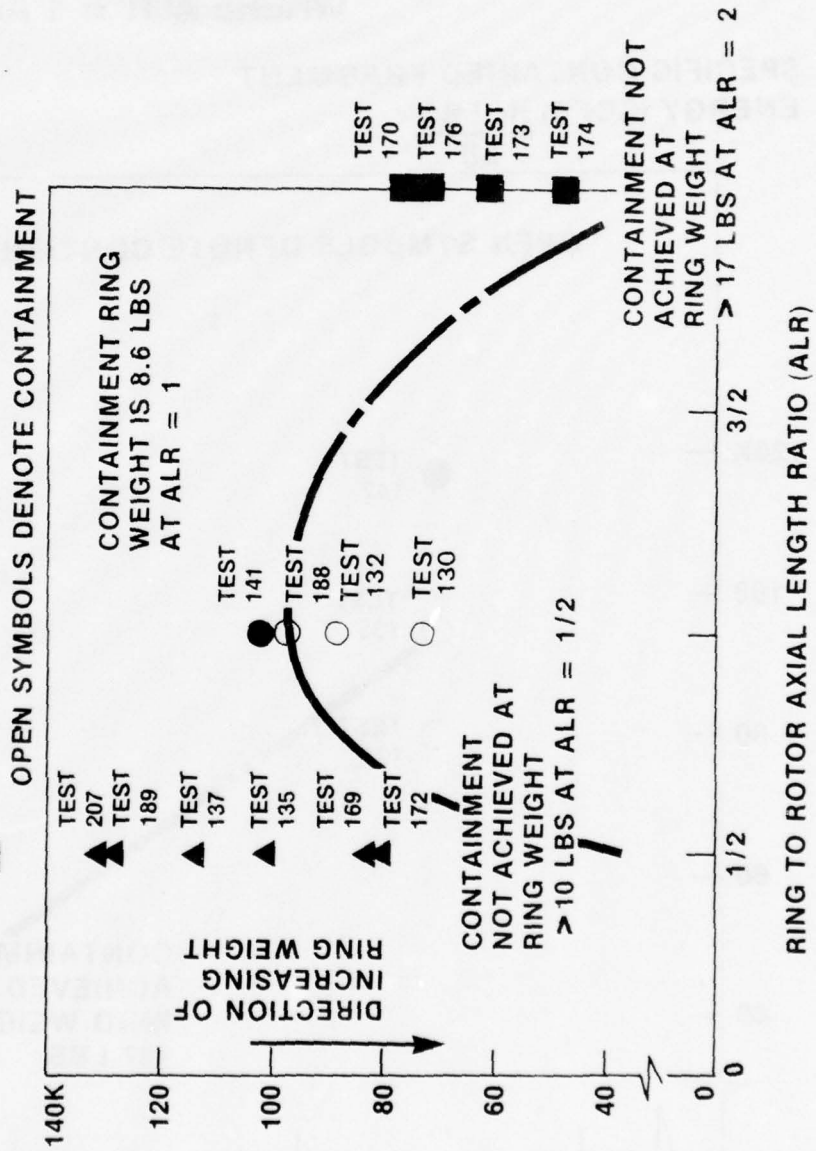


FIGURE 7

SCFE-ALR RELATIONSHIP  
FOR SMALL ROTOR CONTAINMENT  
4130 CAST STEEL RING  
NF = 3

SPECIFIC CONTAINED FRAGMENT  
ENERGY (SCFE) IN-LBS  
LB



### FIGURE 8

SCFE-ID<sub>R</sub> RELATIONSHIP  
4130 CAST STEEL RING

WHERE ALR = 1 AND NF = 2

SPECIFIC CONTAINED FRAGMENT  
ENERGY (SCFE)  $\frac{\text{IN-LBS}}{\text{LB}}$

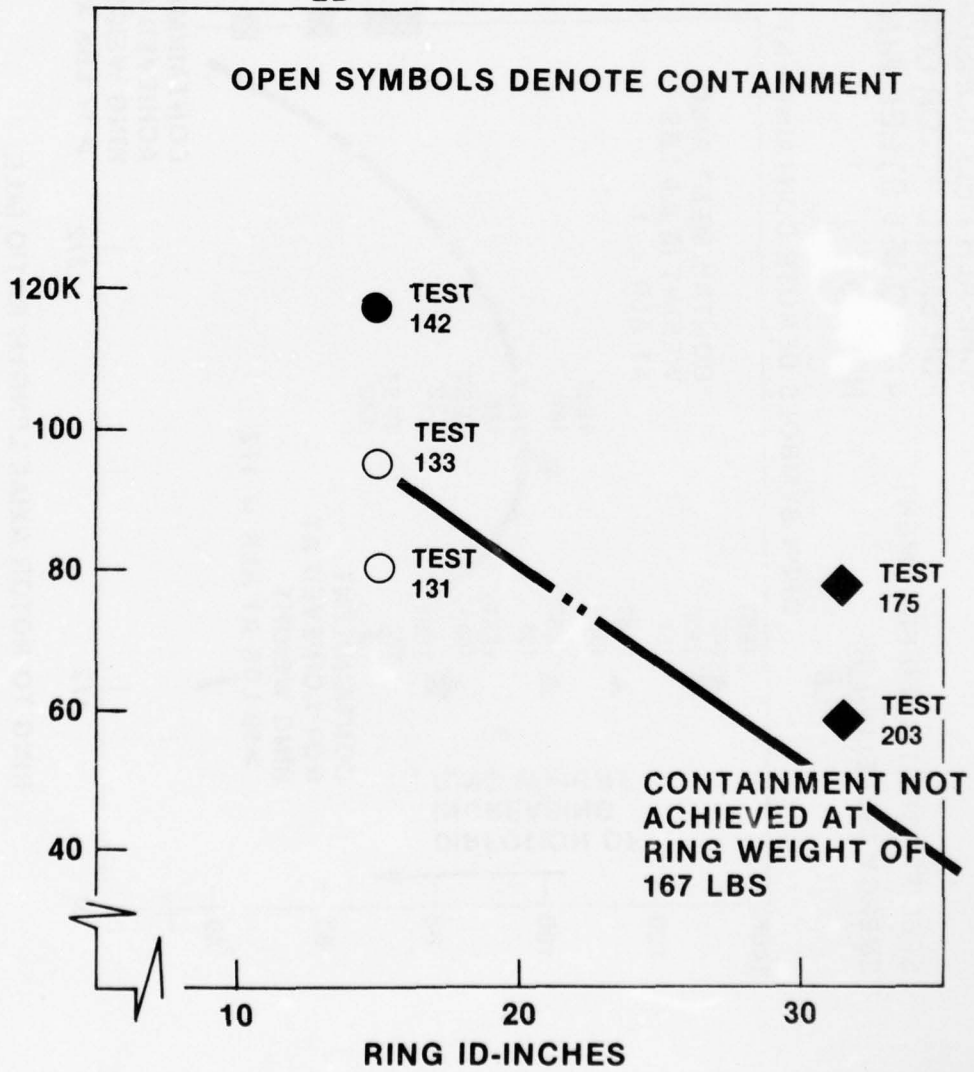
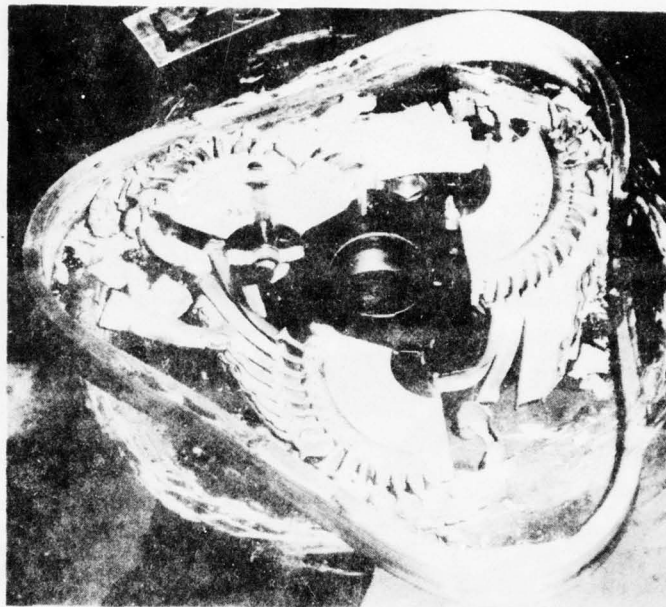
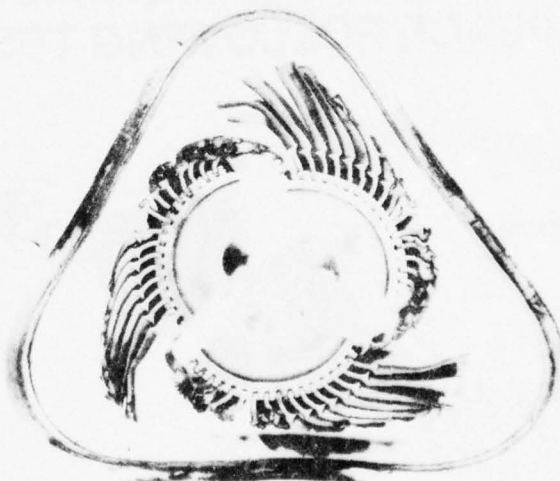


**FIGURE 9**

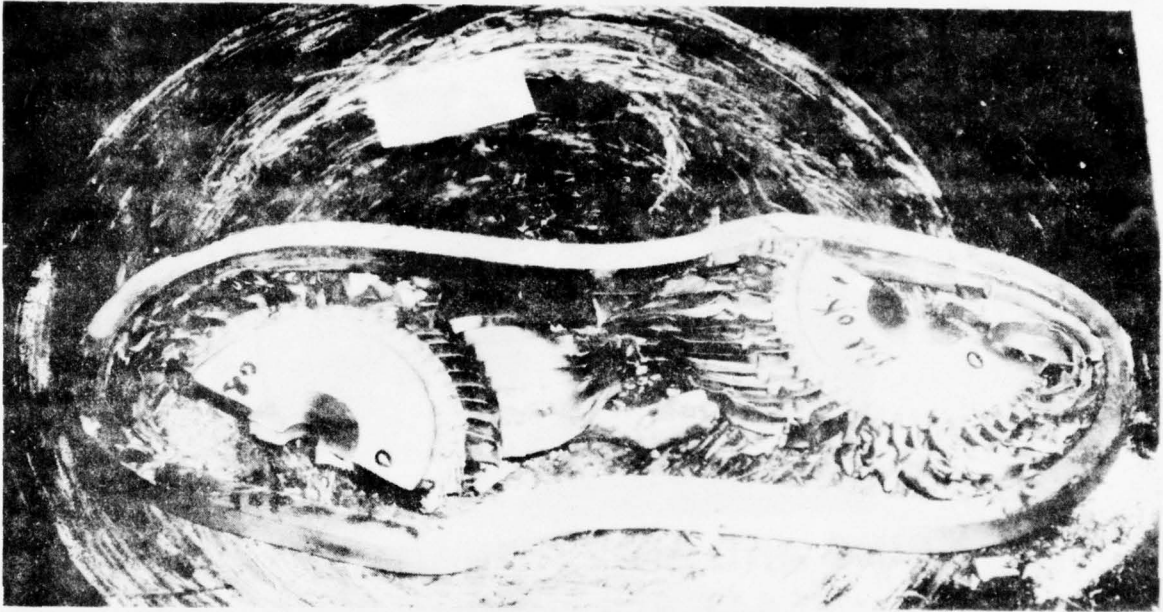


**RING AND ROTOR FRAGMENTS IN PLACE FOLLOWING TEST**



**SMALL ROTOR 3 FRAGMENT  
CONTAINMENT  
POST TEST RESULTS**

**FIGURE 10**

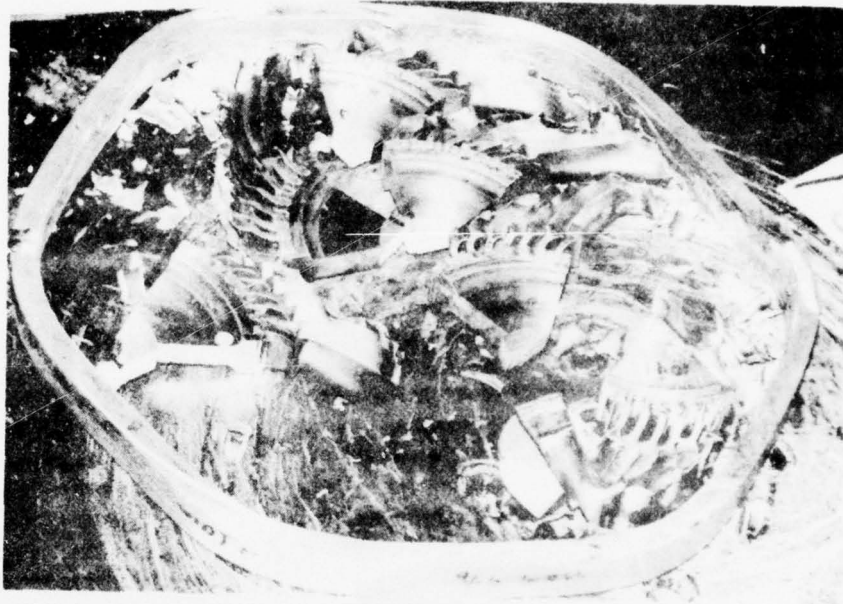


**RING AND ROTOR FRAGMENTS IN  
PLACE FOLLOWING TEST**



**SMALL ROTOR  
2 FRAGMENT CONTAINMENT  
POST TEST RESULTS**

**FIGURE 11**



**RING AND ROTOR FRAGMENTS IN PLACE FOLLOWING TEST**



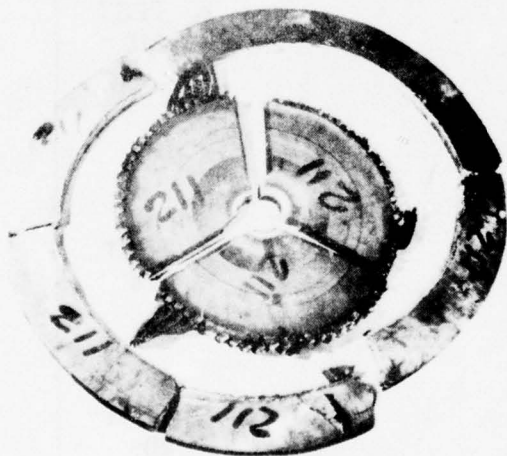
**SMALL ROTOR 6 FRAGMENT  
CONTAINMENT  
POST TEST RESULTS**

FIGURE 12



SMALL ROTOR 2, 3 AND  
6-FRAGMENT CONTAINMENT  
POST TEST RESULTS

**FIGURE 13**



**LARGE ROTOR  
2, 3 AND 6 FRAGMENT  
CONTAINMENT  
POST TEST RESULTS**

**FIGURE 14**

**SCFE-NF RELATIONSHIP  
FOR LARGE ROTOR CONTAINMENT  
4130 CAST STEEL RING  
ALR = 1**

**SPECIFIC CONTAINED FRAGMENT  
ENERGY (SCFE) IN-LBS  
LB**

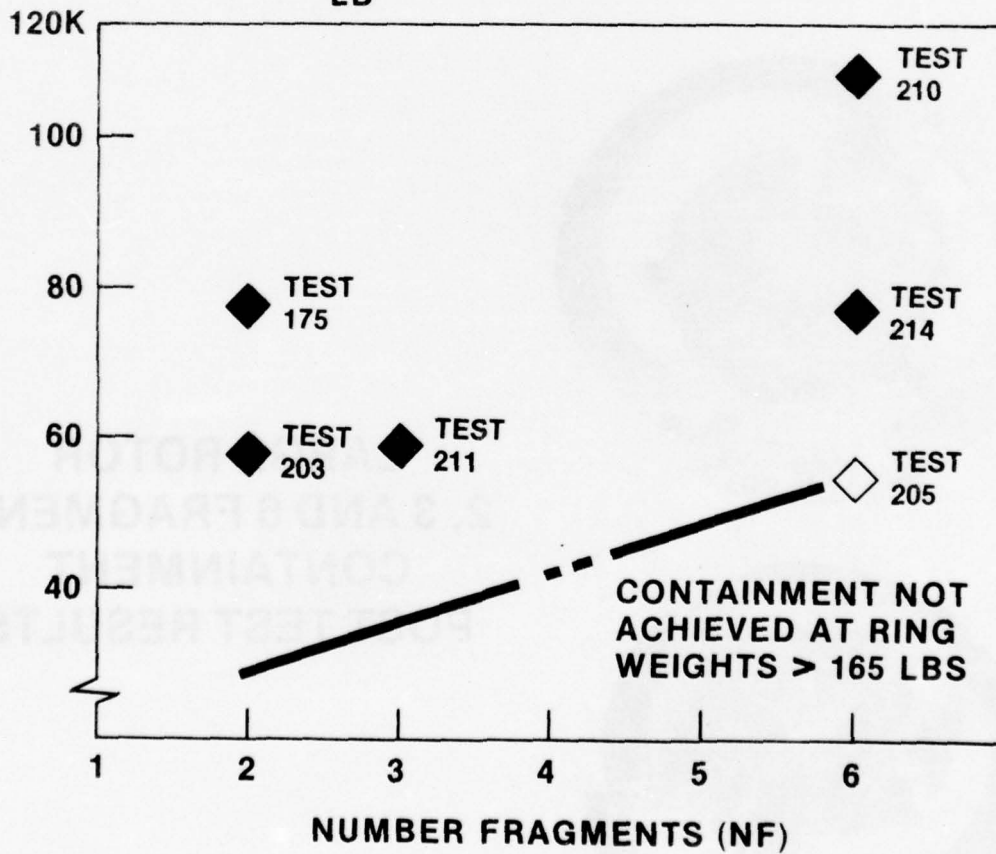


### FIGURE 15

#### SCFE-ALR RELATIONSHIP FOR LARGE ROTOR CONTAINMENT 4130 CAST STEEL RING NF = 2

SPECIFIC CONTAINED FRAGMENT  
ENERGY (SCFE) IN-LBS

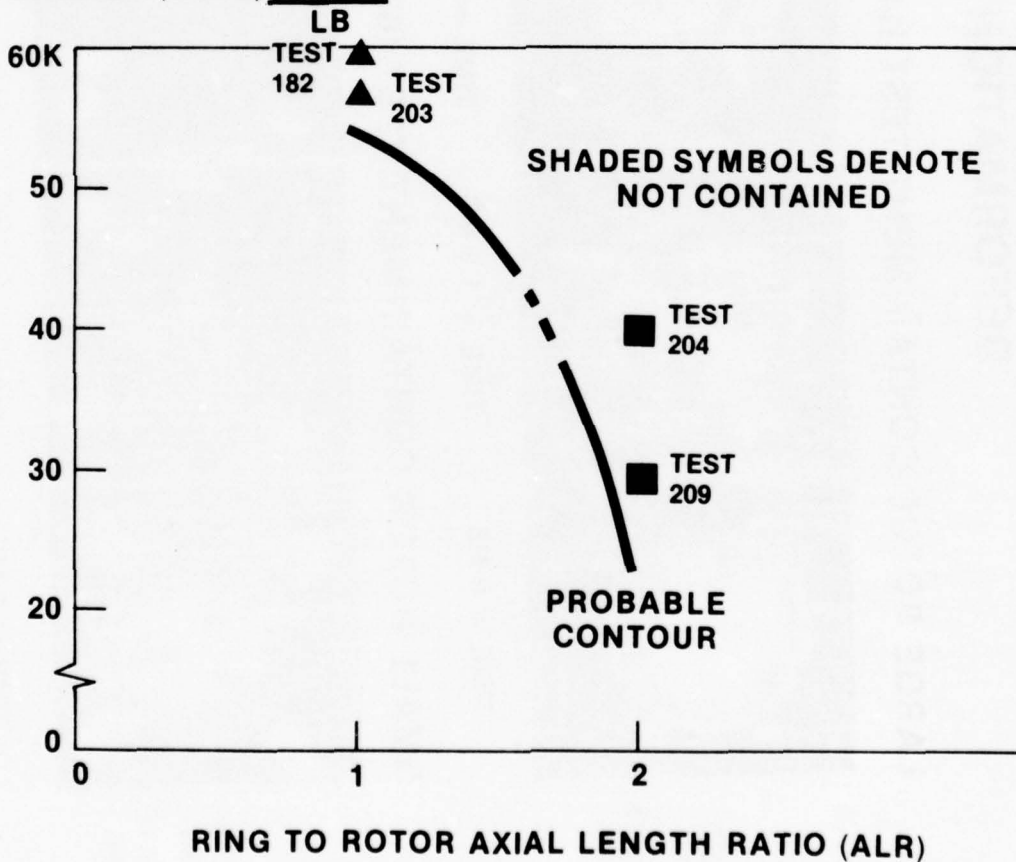
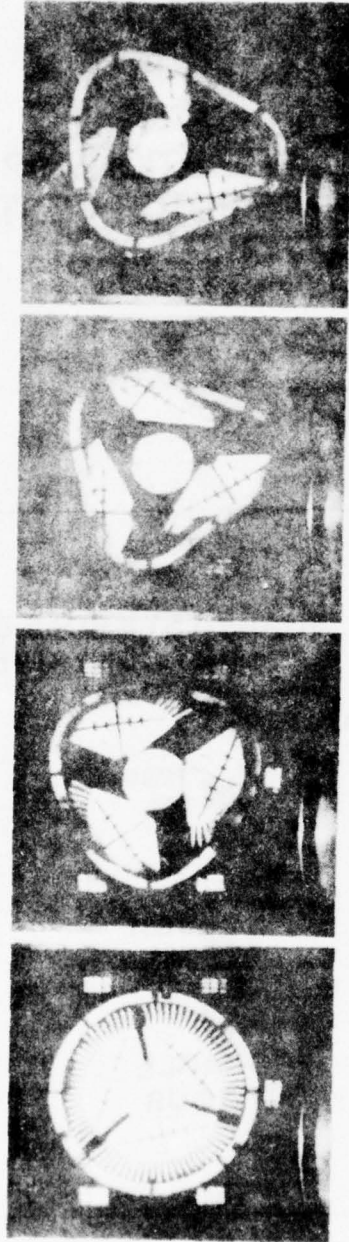


**FIGURE 16**  
**ROTOR BURST FRAGMENT**  
**CONTAINMENT RING**  
**DEFORMATION CHARACTERISTICS**

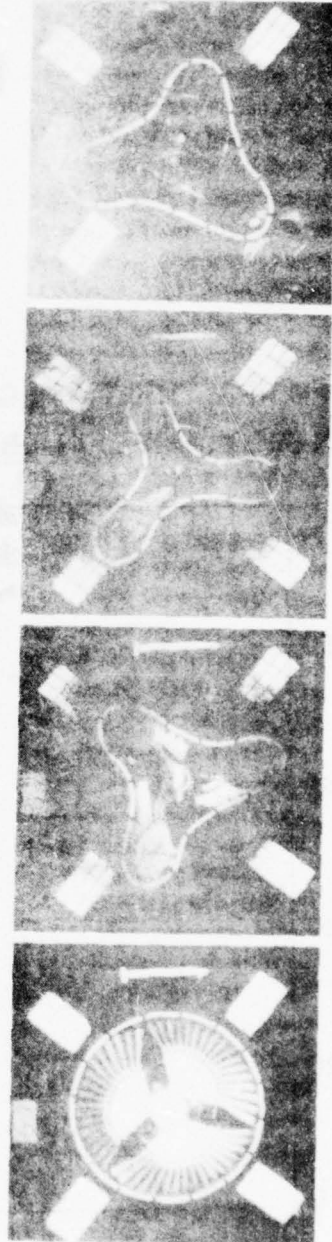
**LARGE ROTOR CONTAINMENT TEST (145)**



ROTOR DIA:  
30.6 IN.  
BURST SPEED:  
6311 RPM  
FRAMING RATE:  
15320 PPS

TIME = 0 MS      TIME = 1.9 MS      TIME = 3.7 MS      TIME = 5.9 MS

**SMALL ROTOR CONTAINMENT TEST (67)**



ROTOR DIA:  
14.0 IN.  
BURST SPEED:  
18829 RPM  
FRAMING RATE:  
14821 PPS

TIME = 0 MS      TIME = 1.7 MS      TIME = 2.8 MS      TIME = 5.5 MS

**FIGURE 17**



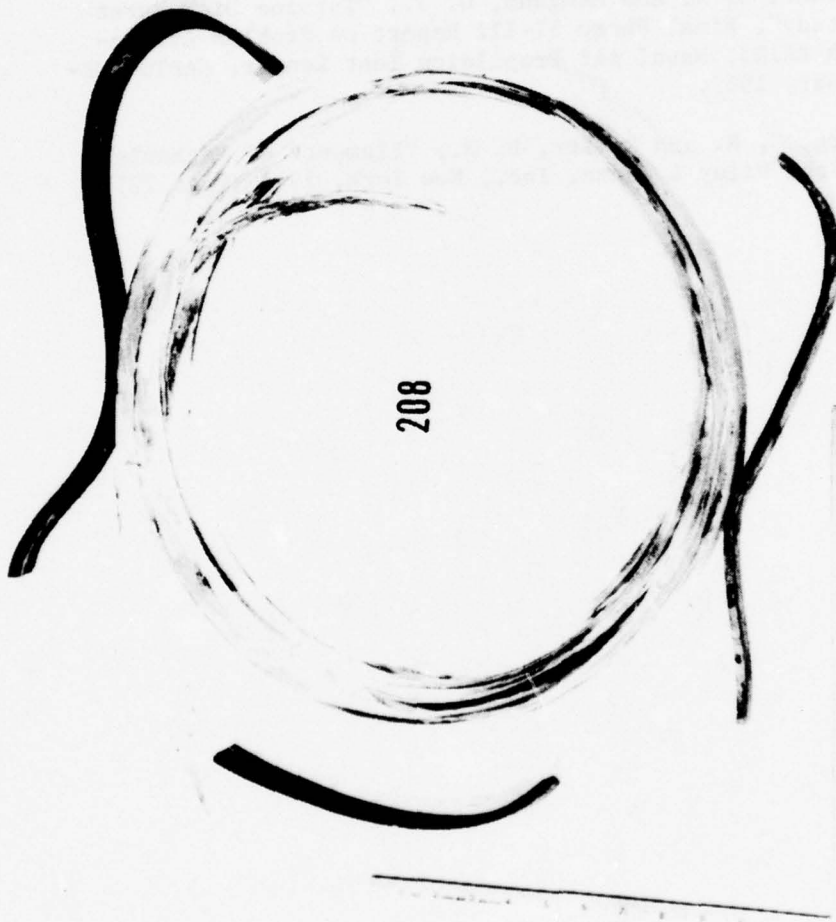
**SMALL ROTOR 3 FRAGMENT  
CONTAINMENT WITH A  
FIBERGLASS RING  
POST TEST RESULTS**

**FIGURE 18**



**SMALL ROTOR 3 FRAGMENT  
CONTAINMENT WITH A BORON  
CARBIDE/FIBERGLASS  
COMPOSITE RING  
POST TEST RESULTS**

**FIGURE 19**



**SMALL ROTOR 3 FRAGMENT  
CONTAINMENT WITH A STEEL/  
FIBERGLASS COMPOSITE RING  
POST TEST RESULTS**

NAPTC-PE-98

REFERENCES

1. REPORT - Mangano, G. J., "Rotor Burst Protection Program - Phases VI and VII; Exploratory Experimentation to Provide Data For The Design of Rotor Burst Fragment Containment Rings", Naval Air Propulsion Test Center, NAPTC-AED-1968 of March 1972
2. REPORT - Martino, A. A. and Mangano, G. J., "Turbine Disk Burst Protection Study", Final Phase II-III Report on Problem Assignment NASA DPR #R105, Naval Air Propulsion Test Center, NAPTC-AEL-1848 of February 1967.
3. TEXT - Freberg, C. R. and Kemler, E. N., "Elements of Mechanical Vibration", John Wiley & Sonce, Inc., New York, 1949 (Page 23).

NAPTC-PE-98

APPENDIX A

Rotor Burst Protection Program  
Experimental Test Data Compilation

DATA COMPILATION NOTES:

- (1) GE T58 Engine Power Turbine Rotor - Refer to Figure A-1 for dimensional and physical details.
- (2) SRCT Ring Diameter = 15.0 inches.
- (3) NF - Centrifugally cast 4130 steel billet produced by National Forge Company, refer to Figure A-2 for stress-strain char.
- (4) ACIPCO - Centrifugally cast 4130 steel billet produced by ACIPCO, refer to Figure A-3 for stress-strain char.
- (5) Fiber Glass - Composite ring manufactured by Eshbaugh Corporation; construction - E-glass roving in an epoxy resin matrix.
- (6) B/C-Glass - Composite ring manufactured by Reflective Laminates/Fansteel; construction - Boron Carbide segments backed with E-glass tape in an epoxy resin matrix (see Figure A-4).
- (7) STL-Glass - Composite ring; construction-4130 plate steel segments backed with E-glass roving in an epoxy matrix (see Figure A-5).
- (8) Curtiss-Wright J65 Engine Stage 2 Turbine Rotor; Refer to Figure A-6 for dimensional and physical details.
- (9) LRCT Ring Diameter = 31.64 inches.
- (10) Centrifugally cast 4130 steel billet produced by ACIPCO. Refer to Figure A-7 for stress-strain char.
- (11) C - Contained  
NC - Not Contained

SMALL ROTOR (1) CONTAINMENT TESTS (SRCT):

TEST NO.	RING DATA (2)				ROTOR DATA			RESULTS	
	AXIAL LENGTH IN	RADIAL THICKNESS IN	WEIGHT LBS	MATERIAL	NO. FRAGMENTS	BURST SPEED RPM	BURST ENERGY IN-LBS	SCFE IN-LBS/LB	CONT. COND.
129	1.0	0.560	7.68	NF(3)	2	18,630	722,424.0	94,065.6	NC
131	1.0	0.750	10.44	NF	2	20,022	834,413.6	79,924.7	C
133	1.0	0.625	8.63	NF	2	19,899	824,193.1	95,503.3	C
142	1.0	0.5625	7.77	NF	2	20,889	908,242.4	116,890.9	NC
126	1.0	0.250	3.41	NF	3	19,754	799,831.1	234,554.6	NC
127	1.0	0.375	5.14	NF	3	19,720	797,080.2	155,074.0	NC
128	1.0	0.507	7.0	NF	3	19,665	792,640.2	113,234.3	NC
130	1.0	0.750	10.49	NF	3	19,416	772,694.3	73,660.1	C
132	1.0	0.625	8.67	NF	3	19,342	766,815.6	88,444.7	C
138	1.0	0.625	8.62	NF	3	21,363	935,433.0	108,518.9	C
139	1.0	0.561	7.76	NF	3	18,897	731,937.4	94,321.8	NC
141	1.0	0.561	7.78	NF	3	19,719	796,999.4	102,442.1	NC
188	1.0	0.625	8.72	ACIPCO(4)	3	20,347	848,572.5	97,313.4	C
134	1.0	0.625	8.60	NF	6	20,056	786,168.2	91,414.9	C
136	1.0	0.5625	7.69	NF	6	19,775	764,292.8	99,387.9	C

SMALL ROTOR (1) CONTAINMENT TESTS (SRCT):

TEST NO.	RING DATA (2)			ROTOR DATA			RESULTS		
	AXIAL LENGTH IN	RADIAL THICKNESS IN	WEIGHT LBS	MATERIAL	NO. FRAGMENTS	BURST SPEED RPM	BURST ENERGY IN-LBS	SCFE IN-LBS/LB	CONT. COND.
140	1.0	0.500	6.89	NF	6	20,420	814,963.7	118,282.1	NC
135	0.5	1.200	8.56	NF	2	20,437	869,362.2	101,561.0	C
137	0.5	1.075	7.71	NF	2	20,559	879,772.7	114,108.0	(a)
168	0.5	1.402	10.17	NF	3	19,164	752,766.9	74,018.4	C
169	0.5	1.352	9.81	NF	3	20,000	819,976.0	83,575.5	NC
172	0.5	1.394	10.18	NF	3	19,978	818,073.3	80,360.8	NC
177	0.5	0.868	6.20	NF	3	19,103	747,982.4	120,642.3	C
178	0.5	0.883	6.13	NF	3	20,975	901,762.5	147,106.4	NC
207	0.5	0.874	6.16	ACPICO	3	19,880	810,067.1	131,504.4	NC
189	0.5	0.885	6.33	ACPICO	3	19,933	814,392.1	128,655.9	NC
170	2.0	0.375	10.81	NF	3	20,243	839,920.0	77,698.4	NC
173	2.0	0.497	13.57	NF	3	20,206	836,852.5	61,669.3	NC
174	2.0	0.6105	17.01	NF	3	20,032	822,501.8	48,354.0	NC
176	2.0	0.432	11.96	NF	3	20,559	866,347.6	72,437.1	NC
143	1.0	1.50	6.03	B/C-GLASS (6)	3	19,058	744,462.5	123,459.8	C

(a) CONTAINMENT QUESTIONABLE - UNDETERMINED

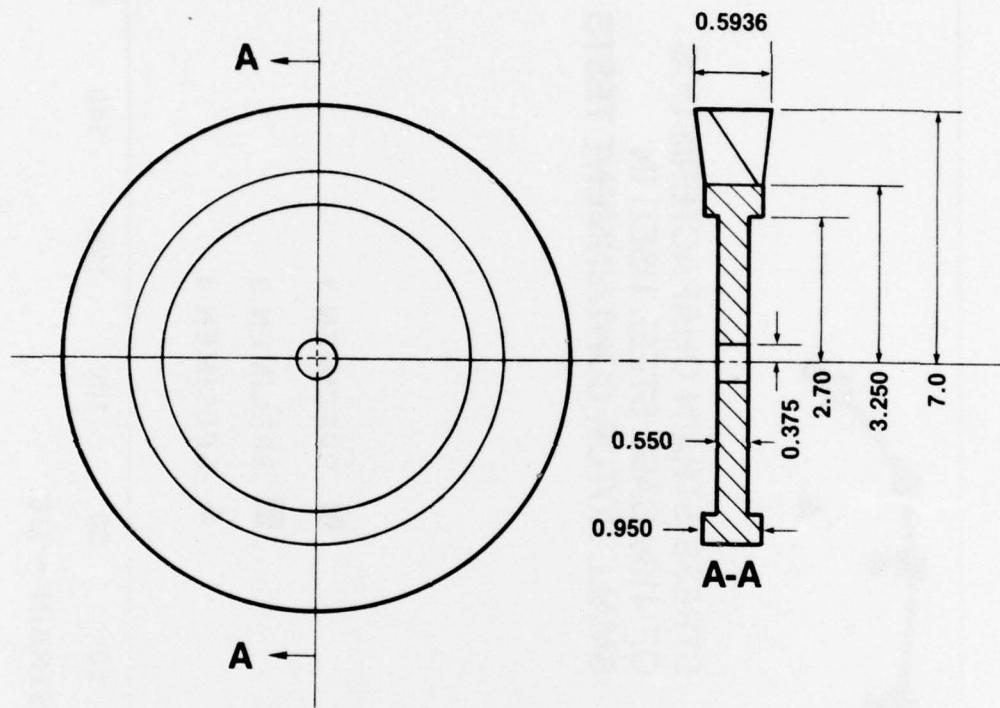
SMALL ROTOR (1) CONTAINMENT TESTS (SRCT):

TEST NO.	RING DATA (2)				ROTOR DATA			RESULTS	
	AXIAL LENGTH IN	RADIAL THICKNESS IN	WEIGHT LBS	MATERIAL	NO. FRAGMENTS	BURST SPEED RPM	BURST ENERGY IN-LBS	SCFE IN-LBS/LB	CONT. COND.
144	1.0	1.375	5.9	FIBER GLASS (5)	3	21,826	976,419.6	165,494.9	NC
208	1.0	1.183	6.88	STL-GLASS (7)	3	19,556	783,877.6	113,935.7	NC
183	1.0	1.388	5.4	FIBER GLASS	3	20,680	876,575.4	161,135.2	NC

LARGE ROTOR (8) CONTAINMENT TESTS (LRCT):

TEST NO.	RING DATA (2)				ROTOR DATA			RESULTS	
	AXIAL LENGTH IN	RADIAL THICKNESS IN	WEIGHT LBS	MATERIAL	NO. FRAGMENTS	BURST SPEED RPM	BURST ENERGY IN-LBS	SCFE IN-LBS/LB	CONT. COND.
167	1.25	2.750	105.0	ACIPCO (10)	2	8,044	8,649,195	82,373.2	NC
175	1.25	3.250	125.5	ACIPCO	2	8,581	9,842,544	78,426.6	NC
180	1.25	1.800	70.5	ACIPCO	2	7,798	8,119,958	115,176.7	NC
181	1.25	1.939	74.0	ACIPCO	2	8,592	9,867,795	133,348.5	NC
182	1.25	4.000	160.0	ACIPCO	2	8,416	9,541,828	59,636.4	NC
203	1.25	4.1875	166.6	ACIPCO	2	8,500	9,557,585	57,968.6	NC
211	1.25	4.183	168.25	ACIPCO	3	8,614	9,918,373	58,950.2	NC
205	1.25	4.231	168.75	ACIPCO	6	8,316	9,243,994	54,779.2	C
210	1.25	2.500	95.0	ACIPCO	6	8,764	10,266,808	108,071.6	NC
214	1.25	3.250	123.0	ACIPCO	6	8,458	9,562,381	77,743	NC
204	2.5	3.000	232.0	ACIPCO	2	8,270	9,142,011	39,405	NC
209	2.5	4.225	330.0	ACIPCO	2	8,499	9,655,313	29,259	NC

**FIGURE A-1**



**TYPE ROTOR: T-58 POWER TURBINE (MODIFIED, UNSLOTTED)**

**ROTOR WEIGHT: 11.8 LBS (AVG.)**

**ROTOR INERTIA: 151 LB-IN<sup>2</sup> (NOMINAL)**

	<u>DISK</u>	<u>BLADES</u>
<b>MATERIAL:</b>	A-286	SEL-5
<b>PROPERTIES:</b>		
SU	157K psi	136K psi
SY	110K psi	118K psi
EU	12%	12%
HD	313 BHN	313 BHN

FIGURE A-2

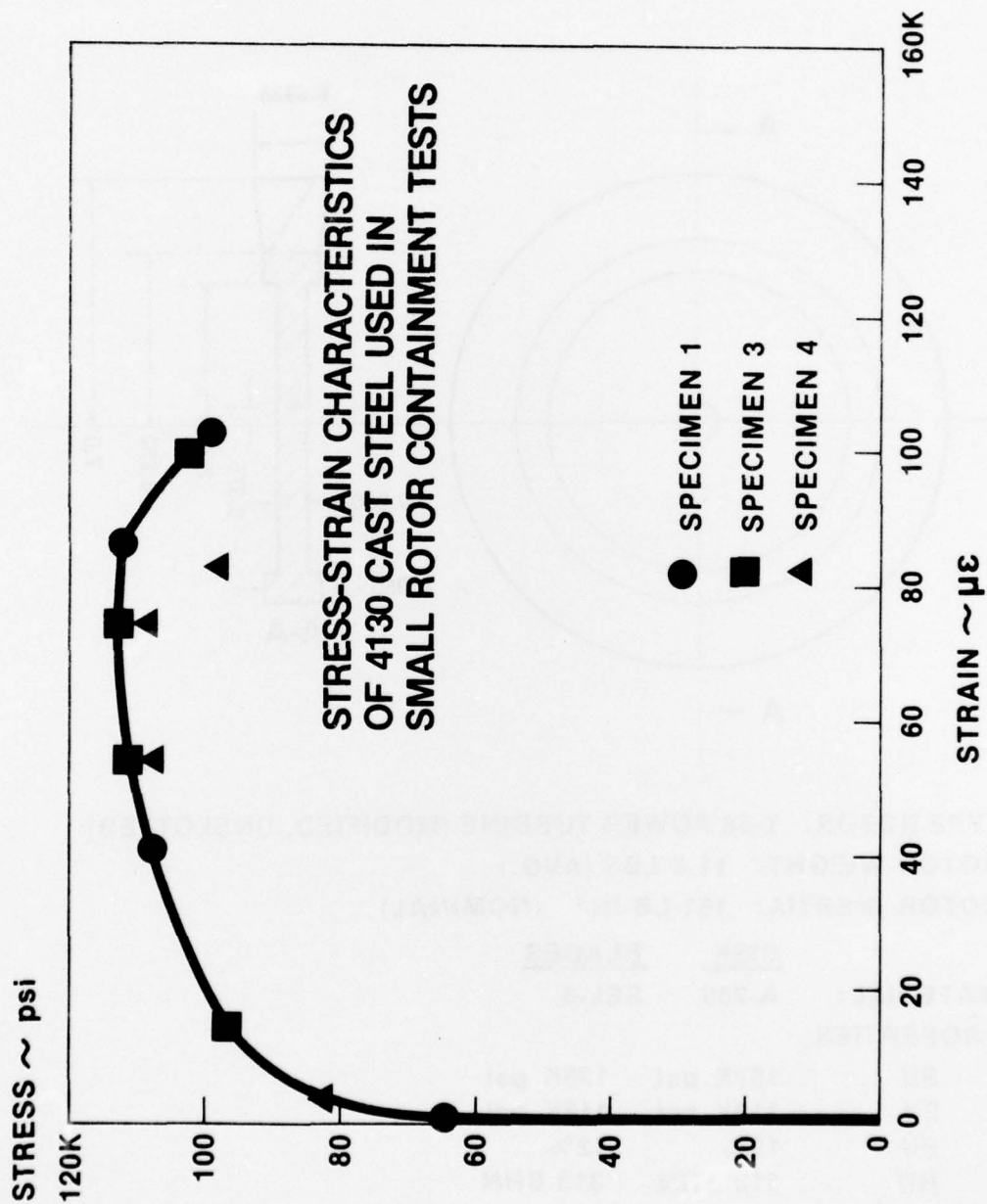
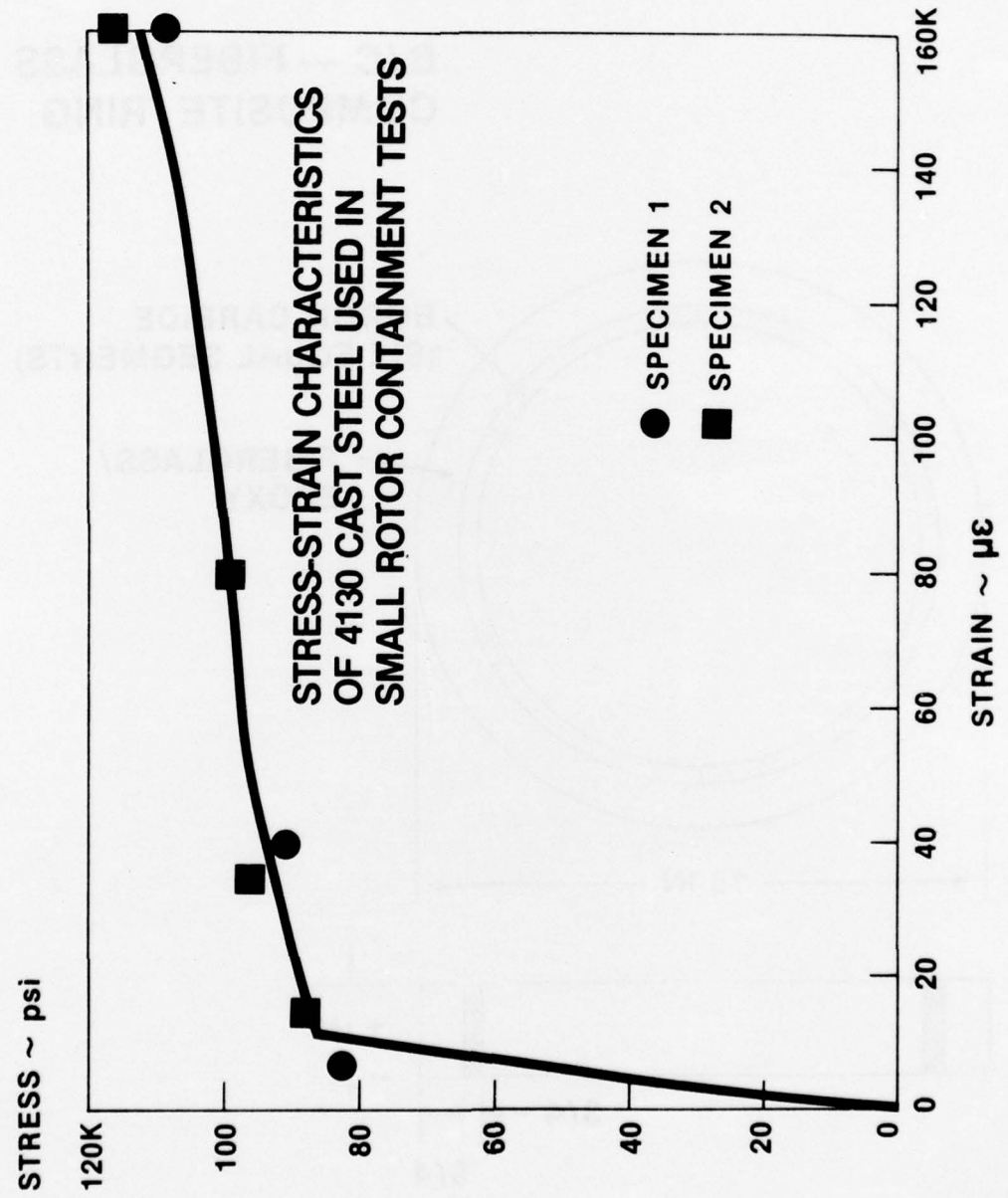
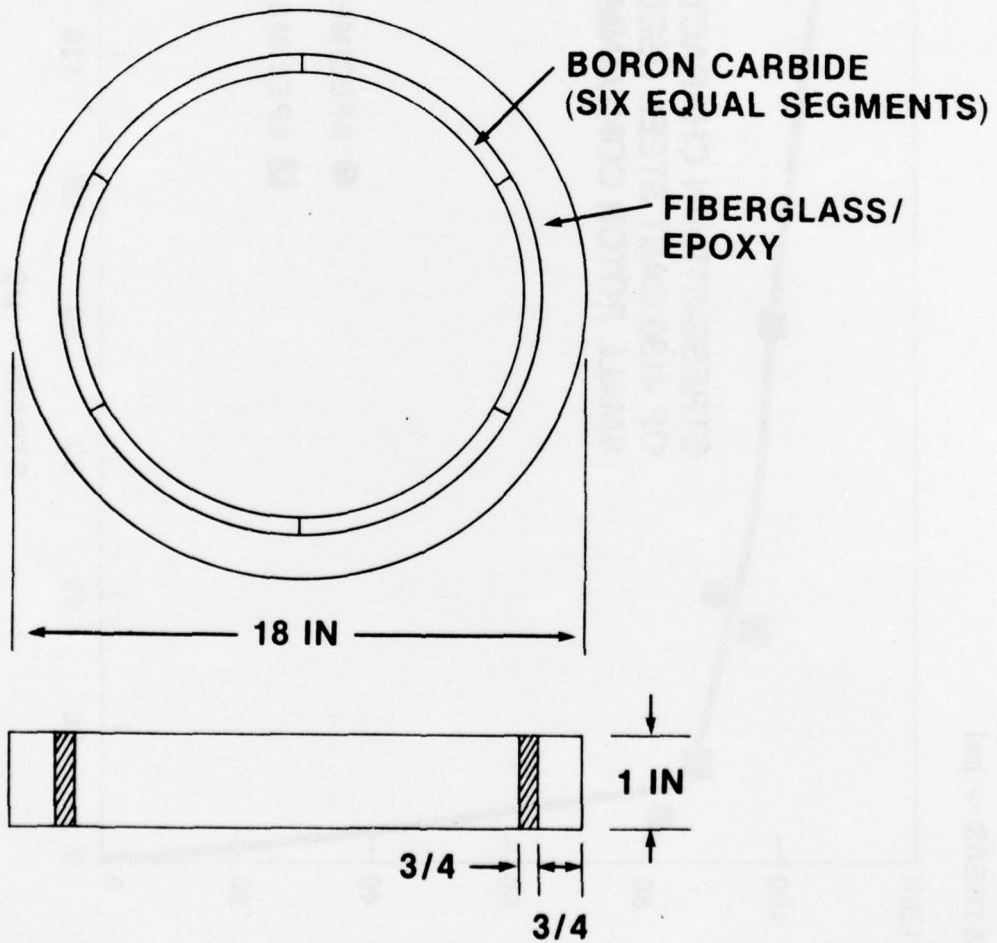


FIGURE A-3



**FIGURE A-4**

**B/C — FIBERGLASS  
COMPOSITE RING**



**FIGURE A-5**

**STL-FIBERGLASS COMPOSITE RING**

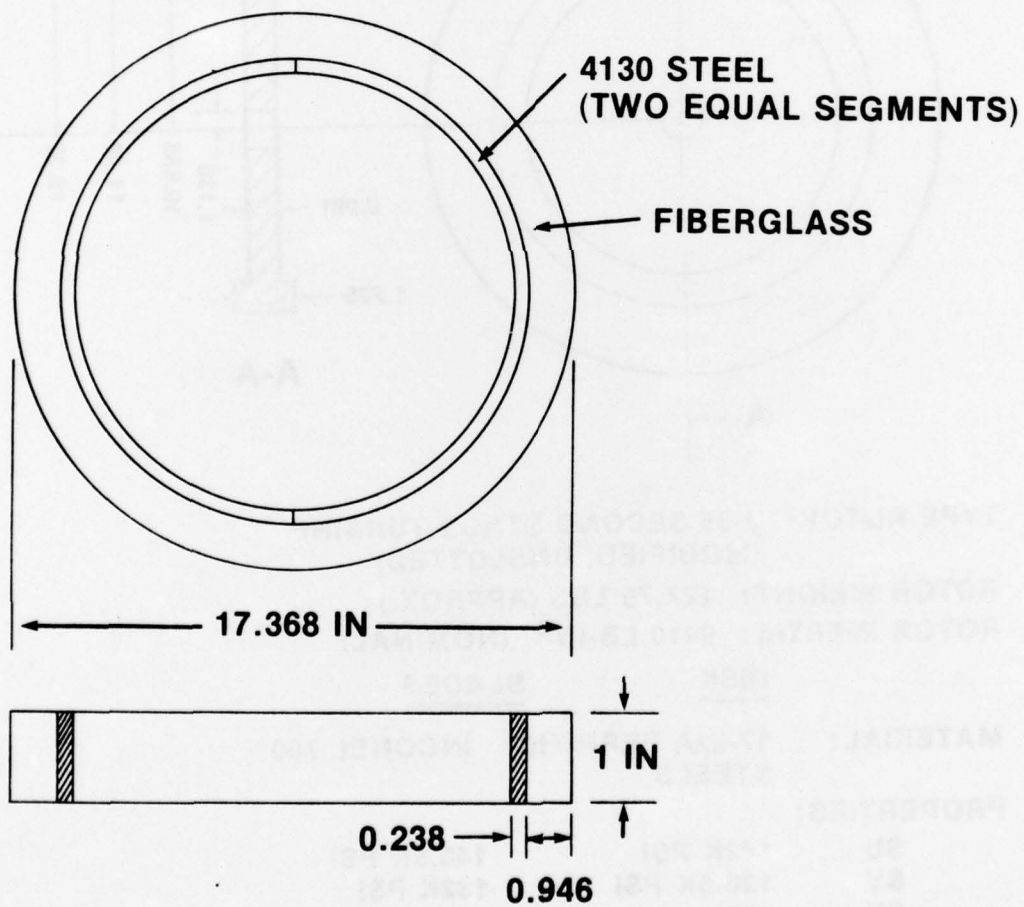
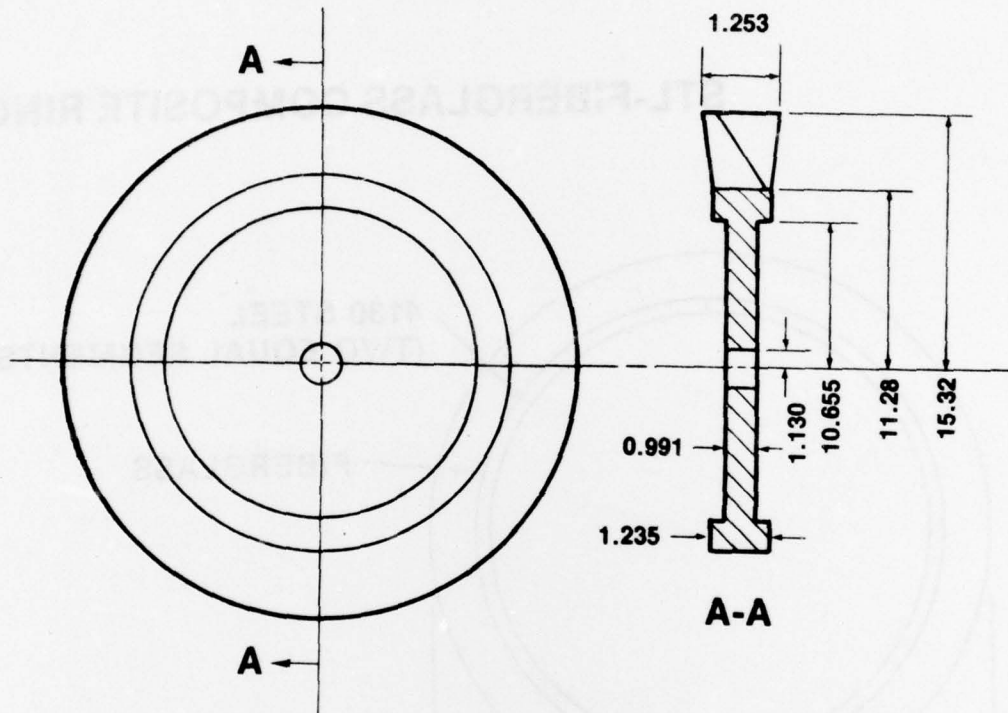


**FIGURE A6**



**TYPE ROTOR: J-65 SECOND STAGE TURBINE  
(MODIFIED, UNSLOTTED)**

**ROTOR WEIGHT: 127.75 LBS (APPROX.)**

**ROTOR INERTIA: 9410 LB-IN<sup>2</sup> (NOMINAL)**

**DISK**

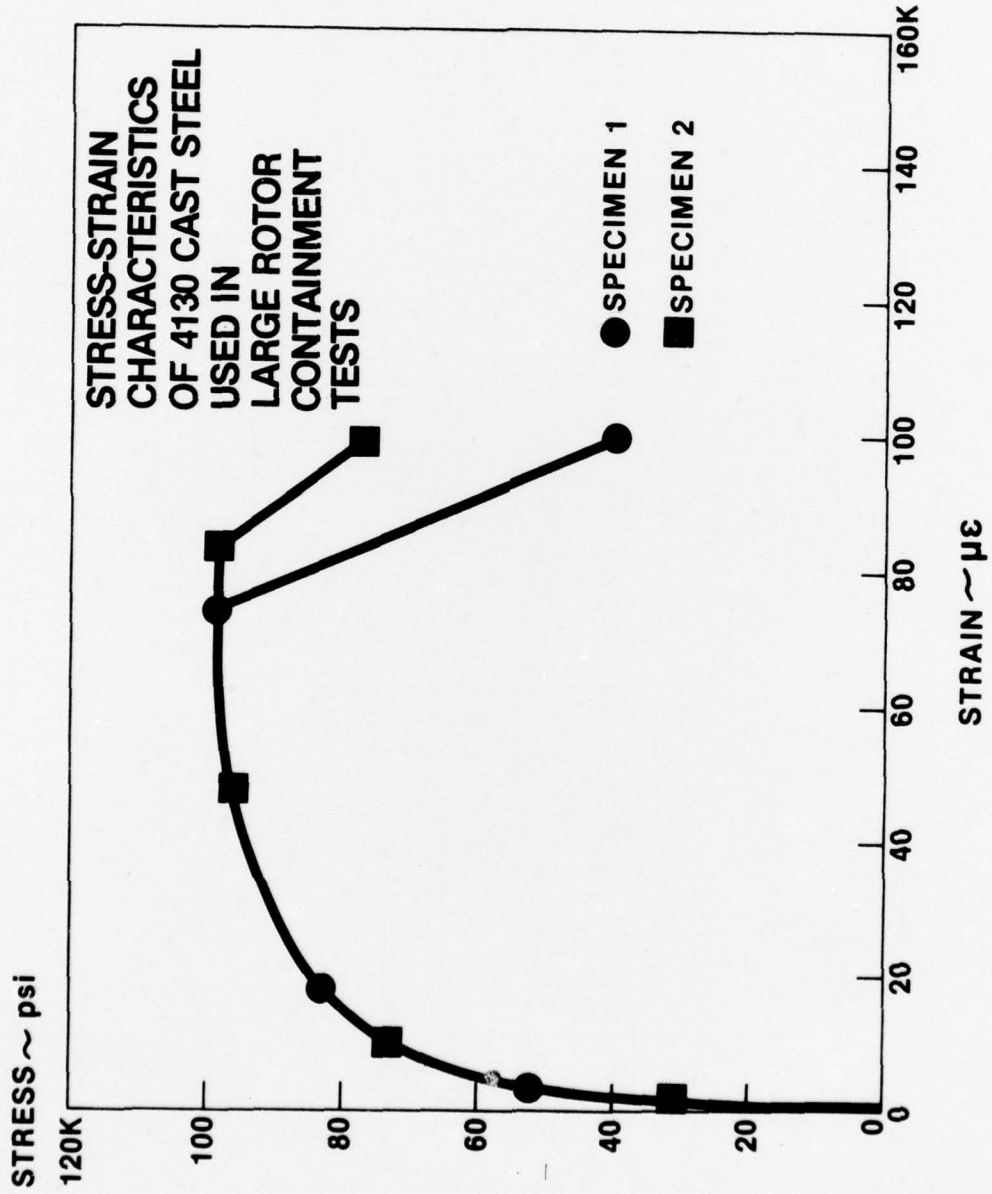
**BLADES**

**MATERIAL: 17-22A FERRITIC INCONEL 700  
STEELS**

**PROPERTIES:**

<b>SU</b>	<b>142K PSI</b>	<b>146.5K PSI</b>
<b>SY</b>	<b>126.5K PSI</b>	<b>132K PSI</b>
<b>EU</b>	<b>18%</b>	<b>18%</b>
<b>HD</b>	<b>311 BHN</b>	<b>311 BHN</b>

FIGURE A-7



DISTRIBUTION LIST

<u>Activity</u>	<u>Copies</u>
Commander, Naval Air Systems Command (AIR-50174), Department of the Navy, Washington, D.C. 20361	9
<u>Intra-command Addresses:</u>	
AIR-330A (1)      AIR-5360 (1)      AIR-5362 (1)	
AIR-530 (1)      AIR-5361 (1)      MAT-03L (1)	
AIR-536 (1)	
Commander, Naval Air Development Center, Warminster, PA 18974	1
Commanding Officer, Naval Air Engineering Center, Lakehurst, NJ 08733	1
Commanding Officer, Naval Aviation Safety Center, Naval Air Station, Norfolk, VA 23511	1
Director, Eustis Directorate, U.S. Army Air Mobility Research and Development Laboratory (SAVDL-EU-TAP), Fort Eusits, VA 23604	1
Commanding General, U.S. Army Aviation Systems Command (AMSAV-ERP), 12th and Spruce Streets, St. Louis, MO 63166	1
Commander, Air Force Aeropropulsion Laboratory (AFSC), Wright-Patterson Air Force Base, Dayton, OH 45433	1
National Aeronautics and Space Administration (MS 6-2, MS 49-1, MS 60-3, MS 5-5, MS 3-19, MS 500-302), Lewis Research Center, 21000 Brookpark Road, Cleveland, OH 44135	12
National Aeronautics and Space Administration (RF, RO(2), RLC), Washington, D.C. 20546	4
Federal Aviation Administration (RD-723), Washington, D.C. 20533	1
Defense Documentation Center for Scientific and Technical Infor- mation, Building No. 5, Cameron Station, Alexandria, VA 22314	12
Aeroelastic Laboratory, Massachusetts Institute of Technology, Cambridge, MA 02139	4